EFFECTS OF EPIDERMAL GROWTH FACTOR ON ADULT NEURAL STEM CELLS

Olle Lindberg

2013

UNIVERSITY OF GOTHENBURG

Center for brain repair and rehabilitation

Department of Clinical Neuroscience and Rehabilitation

Institute of Neuroscience and Physiology

At Sahlgrenska Academy

Cover illustration: Graphical illustration of epidermal growth factor-induced polyp in the adult rat subventricular zone

The most exciting phrase to hear in science,

the one that heralds new discoveries,

is not 'Eureka!' but 'That's funny...'

Isaac Asimov

ABSTRACT

In the adult brain neural stem cells are present in two discrete regions; the hippocampus and the subventricular zone (SVZ). The environment surrounding the stem and progenitor cells, the neurogenic niche, is integral for proper stem cell development and proliferation. Manipulation of the neurogenic niche provides possibilities in regenerative therapy and modeling of diseases. Epidermal growth factor (EGF) is a growth factor involved in a plethora of developmental and homeostatic processes in the body. In the brain, EGF appears to play a role inducing lineage progression of stem cells to proliferative progenitor cells. Treatment with EGF leads to increased proliferation and expansion of the SVZ and focal hyperproliferative polyps are formed. However, neuroblasts development and neurogenesis are negatively affected.

The current thesis demonstrates how the EGF-induced polyps go through discrete stages of development. Polyps persistently recruit blood vessels and the angiogenic process is preceded by microglia accumulation and apoptosis.

The response of the SVZ to EGF is context dependent. Infusion into the juvenile brain yields a response distinct from the adult brain. Furthermore, prior postnatal whole brain irradiation alters certain aspects of EGF stimulation.

The rostral migratory stream (RMS) is the migratory path used by neuroblasts to reach the olfactory bulb where the cells become mature neurons. Upon EGF treatment the RMS responds in a fashion similar to the SVZ, with reduced numbers of neuroblasts and expansion of immature glial cells. Newly formed cells in the EGF-treated RMS express a unique combination of proteins and display migratory properties.

In summary, this thesis determines new pleiotropic effects of EGF on the SVZ and RMS neurogenic niches, depending on age, length of treatment, and prior radiation therapy. The local microenvironment of the EGF induced-polyps, promoting dysplasia, microglia accumulation, and angiogenesis, can provide important insight into future therapies and diseases modeling of stem cell-related diseases.

POPULÄRVETENSKAPLIG SAMMANFATTNING

Stamceller skiljer sig i flera avseenden från de mogna celler, som till huvuddelen utgör vår kropp. I fosterutvecklingen är det stamceller som kontinuerligt förser det växande fostret med celler som ger upphov till alla celltyper och organ. Hos vuxna är antalet stamceller avsevärt mindre, men spelar en avgörande roll i kroppens underhåll genom att ersätta skadade och åldrande celler. Även i den vuxna hjärnan återfinns stamceller. Dessa celler ger upphov till neuron (nervceller), astrocyter, och oligodendrocyter (gliaceller). Neuronen bildar ett nätverk som skickar elektriska impulser i hjärnan, en process som regleras av astrocyter. Oligodendrocyterna är ansvariga för att skapa isolerande skidor runt nervtrådarna för att underlätta fortplantningen av de elektriska signalerna. Studier av den process genom vilken stamceller utvecklas till mogna, fungerande celler, skulle kunna leda till utveckling av nya terapiformer. Många sjukdomar som drabbar hjärnan, som Alzheimers sjukdom, stroke och Parkinsons sjukdom, leder till förlust av celler. Genom att stimulera de stamceller som finns i hjärnan att ersätta de förlorade cellerna skulle många av sjukdomarnas negativa effekter minskas.

I denna avhandling studeras effekter av tillväxtfaktorn epidermal growth factor (EGF) på neurala stamceller i den unga och vuxna hjärnan. När stamceller i hjärnans ventrikelväggar stimuleras med EGF sker det en kraftig tillväxt av antalet celler. Dessa nybildade celler skiljer sig från de stamceller som normalt finns i detta område. Istället för att utvecklas till unga nervceller liknar de celler som uppstår efter EGF-stimulering omogna gliaceller. De omogna cellerna bildar tumörliknande utväxter från ventrikelväggen och skapar nya blodkärl efter långvarig behandling med EGF. Innan blodkärl bildas i utväxterna invaderas de av mikroglia (hjärnans immunceller) som verkar spela en aktiv roll i blodkärlstillväxten.

I den normala råtthjärnan rör sig celler som bildas i ventrikelväggarna till hjärnans luktcentrum, där de bildar nya neuron. Denna migration av unga nervceller påverkas negativt av EGF-behandling. Istället skapas nya gliaceller längs med det stråk utmed vilka de unga nervcellerna normalt migrerar. Även de

nybildande cellerna kan förflytta sig längs med detta stråk.

I avhandlingen beskrivs dessutom hur EGF kan stimulera stamceller i den strålbehandlade hjärnan. Strålbehandling minskar antalet stamceller i hjärnan, och försämrar även funktionen hos de överlevande stamcellerna. Behandling med EGF kan stimulera den strålbehandlade stamcellszonen i hjärnans ventrikelväggar till att växa, men också skapa utväxter innehållande aktiva stamceller.

Sammanfattningsvis ger avhandlingsarbetet insikt i effekter av EGF-stimulering på stamcelltillväxt och migration. Resultaten bidrar till att öka förståelsen för hur stimulering av neurala stamceller kan användas i terapisyfte, men visar också hur stamceller kan uppvisa egenskaper som skulle kunna representera tidig tumörutveckling.

LIST OF ORIGINAL PAPERS

This thesis is based on the following original papers:

I.   Lindberg OR, Brederlau A, Jansson A, Nannmark U, Cooper-Kuhn
       C, Kuhn HG.
       Characterization of epidermal growth factor-induced dysplasia in
       the adult rat subventricular zone. *Stem Cells and Development.*
       2012 May 20;21(8):1356-66

II.   Lindberg OR, Brederlau A, Kuhn HG.
       Epidermal growth factor-treatment of the adult brain subventricular
       zone leads to focal microglia accumulation and angiogenesis. *In
       manuscript*

III.   Lindberg OR*, Persson Å*, Brederlau A, Shabro A, Kuhn HG
       EGF-Induced Expansion of Migratory Cells in the Rostral
       Migratory Stream. *PLoS One.* 2012;7(9):e46380.

IV.   Lindberg OR, Rosinski M, Kuhn HG.
       Effects of Epidermal Growth Factor on Neural Stem Cells In
       Juvenile and Adult Rats After Postnatal Irradiation. *In manuscript*

*Authors contributed equally to this work

Additional papers not included in this thesis:

Hellström NA, Lindberg OR, Ståhlberg A, Swanpalmer J, Pekny M,
Blomgren K, Kuhn HG.
Unique gene expression patterns indicate microglial contribution
to neural stem cell recovery following irradiation.
Molecular and Cellular Neuroscience. 2011 Apr;46(4):710-9

Hanrieder J, Malmberg P, Lindberg OR, Fletcher JS, and Ewing AG.
Time-of-Flight Secondary Ion Mass Spectrometry based Molecular
Histology of Human Spinal Cord Tissue and Motor Neurons.
Analytical Chemistry. 2013 Sep 17;85(18):8741-8.

Persson Å, Lindberg OR, Kuhn HG
Radixin inhibition decreases adult neural progenitor cell migration
and proliferation in vitro and in vivo. *Frontiers in Cellular
Neuroscience.* 2013 Sep 24;7:161

TABLE OF CONTENTS

ABBREVIATIONS

aCSF	Artificial cerebrospinal fluid
Akt	v-akt murine thymoma viral oncogene homolog 1
AraC	Arabinofuranosyl cytidine
ASM	Acid sphingomyelinase
ATM	Ataxia telangiectasia mutated
ATR	Ataxia telangiectasia and Rad3-related protein
BDNF	Brain-derived neurotrophic factor
bFGF	Basic fibroblast growth factor
bHLH	Basic helix loop helix
BLBP	Brain lipid-binding protein
BSO	Buthionine sulfoximine
BrdU	Bromodeoxyuridine
c-Fos	FBJ murine osteosarcoma viral oncogene homolog
c-Myc	V-myc myelocytomatosis viral oncogene homolog
CaMK	Ca^{2+}/calmodulin-dependent protein kinase
Chk	Checkpoint kinase
CldU	Chlorodeoxyuridine
CNP	2',3'-Cyclic-nucleotide 3'-phosphodiesterase
CNS	Central nervous system
CREB	cAMP response element-binding protein
DAB	3,3'-Diaminobenzidine
DAG	Diacylglycerol
DCX	Doublecortin
DDR	DNA damage response
Dlx2	Distal-less homeobox 2
DNA-PK	DNA-dependent protein kinase
DSB	Double strand break
ECM	Extracellular matrix
EGF	Epidermal growth factor
EGFR	Epidermal growth factor receptor
ErbB	Avian erythroblastosis oncogene B

ERM	Ezrin radixin moesin
FACS	Fluorescence-activated cell sorting
FGF2	Fibroblast growth factor 2
GABA	Gamma-aminobutyric acid
GABA$_A$R	Gamma-aminobutyric acid receptor A
GDP	Guanosine diphosphate
GFAP	Glial fibrillary acidic protein
GFP	Green fluorescent protein
Grb2	Growth factor receptor-bound protein 2
GSK3-β	Glycogen synthase kinase 3 beta
GTP	Guanosine triphosphate
Gy	Gray
HB-EGF	Heparin-binding EGF-like growth factor
Hes5	Hairy and enhancer of split 5
Iba1	Ionized calcium-binding adapter molecule 1
ICV	Intracerebroventricular
Id	Inhibitor of DNA-binding
IdU	Iododeoxyuridine
IP3	Inositol trisphosphate
LIF	Leukemia inhibitory factor
MAPK	Mitogen-activated protein kinase
NeuN	Neuronal nuclei
NG2	Neuron-glial antigen 2
NGF	Nerve growth factor
NHEJ	Non-homologous end joining
NICD	Notch intracellular domain
NO	Nitrous oxide
Olig2	Oligodendrocyte lineage transcription factor 2
OPC	Oligodendrocyte progenitor/precursor cell
p75NTR	p75 neurotrophin receptor
PDGFRα	Platelet-derived growth factor receptor alpha
pERM	Phosphorylated ezrin moesin radixin
PFA	Paraformaldehyde
pHH3	Phospho-histone H3

PI3-K	Phosphatidylinositide 3-kinase
PIP_2	Phosphatidylinositol 4,5-bisphosphate
PIP3	Phosphatidylinositol 3,4,5-trisphosphate
PKB	Protein Kinase B
PKC	Protein Kinase C
PLCγ	Phospholipase C gamma
PSA-NCAM	Polysialylated-neural cell adhesion molecule
Raf-1	RAF proto-oncogene serine/threonine-protein kinase
Ras	Rat sarcoma
RBPj	Recombining binding protein suppressor of hairless
RECA-1	Rat endothelial cell antigen-1
RIBE	Radiation-induced bystander effect
RMS	Rostral migratory stream
Robo	Roundabout
ROS	Reactive oxygen species
RTK	Receptor tyrosine kinase
SEM	Scanning electron microscopy
Sos	Son of Sevenless
Sox2	Sex determining region Y-box 2
SSB	Single strand break
SVZ	Subventricular zone
TAM	Tumor-associated macrophages
TAP	Transit amplifying cell
TBS	Tris-buffered saline
TEM	Transmission electron microscopy
TGF-α	Transforming growth factor alpha
TGF-β	Transforming growth factor beta
TrkB	Tyrosine kinase receptor B
TUNEL	Terminal deoxynucleotidyl transferase dUTP nick end labeling
Wnt	int/Wingless

BACKGROUND

Neural stem cells

Neural stem cells give rise to the central nervous system (CNS) by differentiating into neurons, astrocytes, and oligodendrocytes. Readily present in the developing CNS, stem cells were for a long time thought to be absent from the adult brain (Ramón y Cajal, 1928). The intricate wiring of the neural networks of the adult brain was not expected to benefit from new connections being added. The first evidence of proliferation of neural-like cells came from Joseph Altman, who used tritiated thymidine to study a population of dividing cells in the pre- and postnatal rat brain at different ages (Altman, 1969). Altman demonstrated proliferation occurring in the lateral ventricle walls of postnatal rats. Proliferating cells were also found in the rostral migratory stream (RMS) and the olfactory bulb. Altman tentatively identified labeled cells in the olfactory bulb 20 days after tritiated thymidine injection as endothelial cells, neuroglia, and granule neurons. Kaplan and Hinds went further to study the newly generated cells in the olfactory bulb and hippocampus. Using electron microscopy they confirmed a neuronal identity of the adult-generated cells (Kaplan and Hinds, 1977).

The development of specific neuronal antibodies and the thymidine analog bromodeoxyuridine (BrdU) would later confirm Altman's hypothesis of adult-born neurons in the adult brain (Kuhn et al., 1996). Peter Eriksson and colleagues, using the same methodology, demonstrated the existence of adult neurogenesis in the human hippocampus in the late 1990's (Eriksson et al., 1998). A recently published study very elegantly showed the dynamics of adult neurogenesis in the adult human hippocampus by measuring ^{14}C levels in neurons from post-mortem brains (Spalding et al., 2013). This method makes use of the drastic increases in atmospheric ^{14}C due to above-ground nuclear testing in the 1950's and the sharp decline thereafter, which is reflected in the ^{14}C level of nuclear DNA, thereby "time-stamping" newly generated cells. Measurements of ^{14}C in hippocampal granule cells thus allowed determination of the average age of this cell population. We can now estimate that about 700 new neurons are added to the adult human hippocampus each day, a level comparable to that of rodents.

The neurogenic potential of the second stem cell region of the brain, the subventricular zone (SVZ) was demonstrated in mice by Reynolds and Weiss (1992) and the potential of SVZ as a stem cell reservoir has since been widely studied. However, the neurogenic potential of the human ventricle wall is still uncertain. Structurally distinct from the rodent neurogenic SVZ, proliferative cells exist in the adult human brain (Sanai et al., 2004, Quinones-Hinojosa et al., 2006); however, the functional relevance and extent of adult neurogenesis in the ventricle walls is still not completely established (Curtis et al., 2007, Sanai et al., 2011, Wang et al., 2011, Bergmann et al., 2012).

Neural stem cells in the subventricular zone

The neurogenic niche of the SVZ is situated along the lateral walls of the lateral ventricles, separated from the ventricular space by the ependymal cell layer. Only a few cell layers thick, the SVZ spans a vast area of the adult brain, as it covers the lateral walls of the entire lateral ventricles. Cells are produced throughout the SVZ and progressively make their way rostrally along the ventricle wall towards the rostral migratory stream (RMS) (Lois and Alvarez-Buylla, 1994, Doetsch et al., 1997). The RMS provides a permissive environment for cell migration from the lateral ventricles to the olfactory bulb, where the migrating cells become interneurons (Figure 1)(Luskin, 1993, Merkle et al., 2007). Regional differences exist within the SVZ and the bulk of the proliferative population is found in the rostral parts. The location in the SVZ where a cell is born seems to dictate its prospective function and position in the olfactory bulb (Merkle et al., 2007, Ventura and Goldman, 2007, Young et al., 2007).

All new neurons born in the adult SVZ originate from B-cells. The B-cell is a slowly dividing stem cell with astrocyte-like properties with its developmental origin in radial glia cells of the developing brain (Merkle et al., 2004). The B-cell expresses the glial fibrillary acidic protein (GFAP), often used as a marker for astrocytes (Doetsch et al., 1999a). In the SVZ the B-cell is situated close to the ventricle in the center of a ring of ependymal cells arranged in a pin-wheel structure. The B-cell extends a process between the ependymal cells contacting the ventricle with a single cilia (Figure 1)(Mirzadeh et al., 2008). The opposite end of the B-cell is extending inwards, contacting the vasculature. This poten-

tially means that the B-cell can receive signals from both the cerebrospinal fluid in the ventricle and the vasculature (Tavazoie et al., 2008).

Recent research indicates that several states of B-cell activation exist. The most primitive state is a quiescent state, characterized by GFAP and Hes5 expression. During the second state the B-cell begins to express brain lipid-binding protein (BLBP) and divides more frequently. In the final state, GFAP expression is lost and the B-cell is characterized by epidermal growth factor receptor (EGFR) expression. The progression of the B-cell from early to late states is not continuous, dividing cells can exit the cell cycle and maintain their current state (Giachino et al., 2013). The progeny of the B-cell gives rise to a progenitor cell called a C-cell or transit-amplifying progenitor (TAP) (Doetsch et al., 2002). The C-cell moves from its place of birth close to the ependymal cell layer, towards the underlying vasculature (Figure 1) (Kokovay et al., 2010). The proliferative capability of the C-cell is linked to its proximity to the vasculature and the closer to the vasculature the cells are located, the more frequently the cells divide (Shen et al., 2008, Tavazoie et al., 2008). From this highly proliferative state the C-cells develop into migratory neuroblasts (Doetsch et al., 1997). Neuroblasts migrate in chains rostrally along the entire SVZ. The migratory chains are made up of bundles of neuroblasts, which use each other as substrates and express doublecortin (DCX) and polysialylated neural cell adhesion molecule (Psa-NCAM) (Doetsch et al., 1997, Brown et al., 2003). The chains of migrating cells aggregate in the rostro-dorsal SVZ and are funneled into the RMS (Lois and Alvarez-Buylla, 1994, Lois et al., 1996).

The rostral migratory stream

The final destination of the cells born in the SVZ is the olfactory bulb in the rostral most part of the rodent brain. To reach the olfactory bulb in the rodent brain the neuroblasts must migrate several millimeters, a substantial distance from the perspective of a cell (Luskin, 1993). Unlike the developing brain, most cells in the adult brain are post-mitotic and stationary. As a result, the adult brain is not as permissive towards migration. Furthermore, the structural support in the form of radial glia, used as migratory scaffolds for migratory neural progenitors in the developing brain, is not present in the adult brain (Rakic,

1971). In spite of the very different conditions provided in the adult brain, the RMS shuttles thousands of new cells to the olfactory bulb every day (Lois and Alvarez-Buylla, 1994).

Together, hundreds of migratory chains make up the core of the RMS. Astrocytes ensheath each individual migratory chain, but also form a tube surrounding and possibly separating the entire stream of neuroblasts from the brain parenchyma (Lois et al., 1996, Peretto et al., 2005). Similar to the SVZ, the RMS has its own niche and a population of neural stem cells (Gritti et al., 2002, Alonso et al., 2008, Giachino and Taylor, 2009).

Another important component of the RMS is the network of blood vessels running along the length of the structure. Neuroblasts associate to the blood vessels and use the vasculature as support. The mechanism behind this association is thought to be brain-derived neurotrophic factor (BDNF) signaling. BDNF, synthesized by endothelial cells, binds to the neurotrophin receptor p75NTR expressed by the neuroblasts and promotes blood vessel association (Snapyan et al., 2009). Interestingly, astrocytes also express neurotrophin receptors (TrkB), which can trap extracellular BDNF and regulate the availability of BDNF through $GABA_AR$ (Gamma-aminobutyric acid receptor A)-mediated changes in intracellular calcium levels (Snapyan et al., 2009).

The specialized extracellular matrix (ECM) provides important signaling cues and support for migration in the RMS. ECM molecules, such as laminins and tenascins, are expressed in the developing brain at very high levels. Substantial expression of these molecules persists in the adult RMS (Franco and Muller, 2011). The ECM is believed to stimulate migration both by trapping secreted factors and by direct signaling through integrin receptors. Laminin and the α6β1 integrin stimulate RMS migration, and injection of α6β1-binding amino acids into the striatum diverts neuroblasts from the RMS towards the injection site (Emsley and Hagg, 2003). Blocking of either the α6 or β1 integrin subunit in RMS neuroblasts disrupt migration. Tenascin-C is diffusely expressed in the parenchyma around the primitive RMS in the developing brain. While the RMS forms during the first postnatal weeks, Tenascin-C expression gradually accumulates in the RMS and more specifically around the chains of neuroblasts, indicating an important role of Tenascin-C in adult migration (Peretto et al., 2005).

Other molecules facilitating migration are expressed on the neuroblasts themselves. PSA-NCAM is expressed by neuroblasts in the SVZ. The addition of the PSA moiety to the NCAM molecule putatively facilitates migration by providing additional space between migration cells (Bonfanti, 2006). Mutant mice deficient in NCAM display reduced olfactory bulb size, and wild type neuroblasts transplanted into the mutant RMS fail to migrate (Cremer et al., 1994, Hu et al., 1996). Similar effects can be achieved by enzymatic digestion of PSA alone, suggesting that PSA, and not NCAM, is responsible for the pro-migratory properties of PSA-NCAM (Ono et al., 1994).

Neuroblast migration is not only regulated by factors intrinsic to the SVZ and RMS, but also by factors expressed in other parts of the brain. The chemorepellant protein Slit is produced in the septum and choroid plexus (Hu, 1999, Wu et al., 1999). Slits bind to the Robo receptors expressed by neuroblasts and progenitors in the SVZ. In mice deficient in Slit, SVZ-derived neuroblasts occasionally migrate caudally through the corpus callosum, suggesting a role for Slit/Robo in directing neuroblast migration through the RMS (Nguyen-Ba-Charvet et al., 2004).

An important aspect of neuroblast migration is the rearrangement of the cytoskeletal components of the cell (Cooper, 2013). Doublecortin (DCX) is involved in transporting the microtubule organizing organelle, the centrosome, within the cell as it migrates. In the adult brain, DCX expression is specific for neuroblasts and is therefore one of the most widely used markers for both neuroblasts but also for adult neurogenesis in general (Gleeson et al., 1999, Brown et al., 2003). However, as with most markers, DCX expression is not completely exclusive to neuroblasts. Neurons in the piriform cortex, a region receiving input from the olfactory bulb, reportedly also express DCX (Klempin et al., 2011). In DCX knockout mice, the RMS displays morphological differences compared to wild type, being thicker in the caudal RMS and with fewer cells in the rostral RMS. Although keeping proper direction, neuroblasts migrate at a slower pace and are to a lesser extent able to achieve a correct final position in the olfactory bulb (Koizumi et al., 2006).

Another family of proteins involved in the arrangement of the cytoskeleton and involved in migration is the ERM (Ezrin, Radixin, and Moesin) family of pro-

teins. The ERMs are cytoskeletal linker proteins connecting actin filaments to proteins in the plasma membrane (Kahsai et al., 2006, Valderrama et al., 2012). All three members of the ERM proteins are present in the RMS, however in different cell types. Ezrin is expressed by GFAP-expressing astrocytes, radixin in PSA-NCAM-expressing neuroblasts, and moesin is only weakly expressed in a subset of PSA-NCAM-expressing cells (Persson et al., 2010).
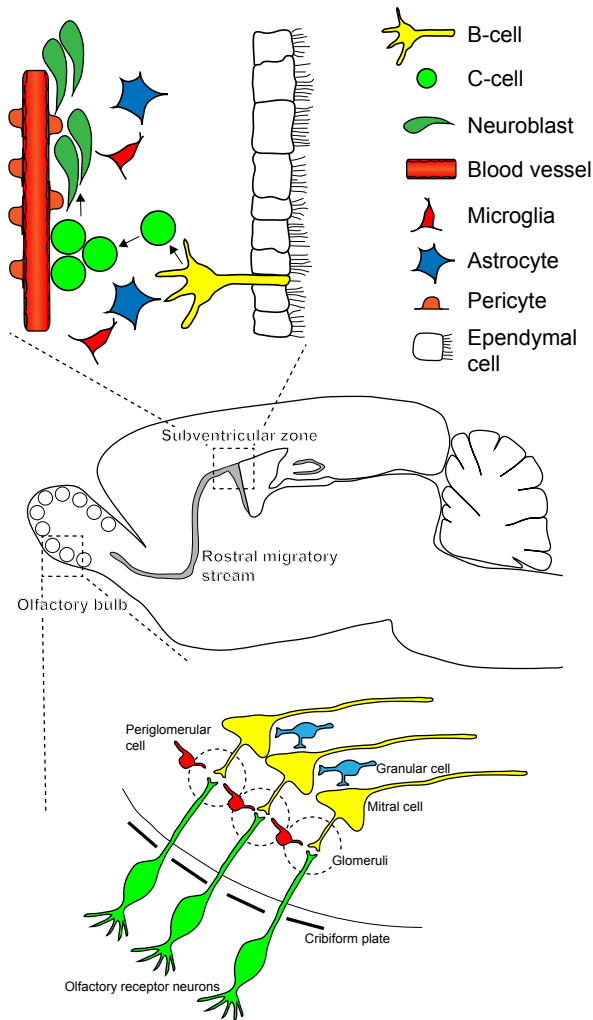
Olfactory bulb

The olfactory bulb is the final destination for the neuroblasts migrating through the RMS. The RMS terminates in the core of the bulb and the neuroblasts switch from a tangential to a radial mode of migration, resulting in a dispersion of migrating cells into the olfactory bulb. One of the most important regulators of this process is reelin (Hack et al., 2002). Addition of exogenous reelin in cell and tissue cultures results in disrupted migratory chains and increased individual cell migration. In the reelin knockout mice *reeler*, neuroblasts accumulate in the core of the bulb, indicating a role of reelin in the tangential to radial migratory transition (Hack et al., 2002). The neuroblasts reaching the olfactory bulb mature into granular and periglomerular interneurons (Figure 1) (Luskin, 1993). Olfactory bulb neuronal sub-type determination and positioning is regulated by the location of the stem cell in the SVZ. The positional identity is preserved following ectopic SVZ transplantation. Additionally, the neuronal identity is kept when SVZ stem cells are expanded and differentiated *in vitro* (Merkle et al., 2007).

Axonal input into the olfactory bulb is relayed from olfactory receptor neurons to mitral and tufted projection neurons (Figure 1). The inhibitory adult-born granular and periglomerular cells are thought to process the sensory input by synapsing in the interface between receptor and projection neurons onto mitral and tufted neurons (Carleton et al., 2003). The integration of new neurons into an existing network provides different challenges compared to neurons that are formed during development. Extensive cell death of young interneurons and specialized sequences of maturation are thought to be mechanisms required for proper integration (Winner et al., 2002). Survival of adult-born neurons is highly activity-dependent and deprivation from olfactory stimuli reduces sur-

vival (Bastien-Dionne et al., 2010). Moreover, activity-dependent survival is also regulated by the age at which the newly born cells receive input. Olfactory training only promotes survival for cells born in a specific interval, since training does not improve survival if performed too early or too late in the development of the newborn neuron (Mouret et al., 2008).

Microglia immune cells play an important role in olfactory bulb adult neurogenesis. Following deafferentiation of olfactory sensory neurons the generation of neurons decreases in the olfactory bulb, but not in the SVZ or RMS. Concomitant with the decrease in newly generated neurons, a reciprocal increase of newly generated microglia can be observed. The decline in neurogenesis following this chemical deafferentiation can be abrogated by preventing microglia activation and proliferation through treatment with the anti-inflammatory drug minocycline (Lazarini et al., 2012). These results suggest an important role of microglial state in regulating the survival of immature neuron in the olfactory bulb.

The functional contribution of adult-born neurons on olfactory perception is still debated. Various methods of adult neurogenesis ablation have been used to study the contribution of adult-born neurons on odor perception and discrimination. The published data are conflicting and the exact role of olfactory bulb adult neurogenesis is unknown (Imayoshi et al., 2008, Lazarini et al., 2009, Sultan et al., 2010, Sakamoto et al., 2011). One suggested role for olfactory bulb adult neurogenesis is to improve separation of similar inputs (Moreno et al., 2009, Sahay et al., 2011b). This process, called pattern separation, is thought to be regulated by adult-born neurons in the hippocampus (Sahay et al., 2011a). Individual odorant receptors can detect multiple odorants and odorants can bind to multiple receptors. However, each odorant binds to a unique combination of receptors (Buck, 2004). Thus, an important aspect of odor perception is to discriminate between similar combinations of activated odorant receptors, a process potentially modulated by adult-bornneurons (Sahay et al., 2011b).

Figure 1. Illustration and overview of the subventricular zone neurogenic niche and the integration of adult-born granular and periglomerular neurons in olfactory bulb

The subventricular zone neurogenic niche

The surrounding environment is vital for proper neural stem cell proliferation and differentiation (Suhonen et al., 1996, Shihabuddin et al., 2000, Seidenfaden et al., 2006). The majority of the non-neurogenic cell types found in the SVZ are involved in maintenance of the neurogenic niche. The vasculature of the SVZ is anatomically and functionally distinct compared to the vasculature in the nearby striatum and corpus callosum. Observing the SVZ vasculature *en face*, from the ventricular surface, reveals a complex vascular network running

parallel to the ependyma. The majority of blood vessels are located at a depth of 10-20μm (Shen et al., 2008). Found closely associated to the endothelial cells are mural cells called pericytes, which are thought to regulate endothelial cell function and permeability. In the SVZ, pericytes contribute to selective permeability of small molecules through the vasculature, allowing passage through the otherwise tightly regulated blood-brain barrier (Tavazoie et al., 2008). Rather than being randomly distributed throughout the vascular bed, progenitor cells in the SVZ appear to aggregate in proliferative clusters close to blood vessels. It has been suggested that these cell aggregates represent a proliferative SVZ sub-niche, much like the one found in the hippocampus (Palmer et al., 2000, Shen et al., 2008). The proliferative niche of the SVZ can partly be explained by a reduced coverage of pericytes, permitting EGFR-expressing C-cells to directly contact endothelial cells (Tavazoie et al., 2008). Another clue to how these proliferative niches are regulated could be through cellular interactions with the ECM. For instance, cells located in close association to laminin-expressing SVZ blood vessels express the laminin receptor α6β1 integrin, indicating an involvement of laminin in homing and retention of progenitor cell in the proliferative vascular niche (Shen et al., 2008). Another ECM component unique to the SVZ neurogenic niche is a specialized basal lamina, lining the outside of the pericyte-covered endothelial cells. So-called fractones, branches of basal lamina, protrude into the extracellular space of the SVZ. Fractones are rich in heparin sulfate proteoglycans and can bind and aggregate growth factors, such as FGFs, EGF and HB-EGF (heparin-binding EGF-like growth factor). The network of fractones is thought to permeate the entire SVZ niche and to regulate stem and progenitor proliferation (Mercier et al., 2002).

Lining the entire cerebroventricular space is the ependymal cell layer, separating the SVZ niche from the ventricles and the cerebrospinal fluid. The individual ependymal cells are tightly associated to the neighboring cells via desmosomes, tight junction, and other junctional complexes (Doetsch et al., 1997). The polarized ependymal cells protrude cilia into the ventricular space, whose main function is to regulate the flow of cerebrospinal fluid through the ventricles. The direction of the flow of cerebrospinal fluid is, in part, involved in regulating neuroblast migration (Sawamoto et al., 2006).

Microglia are found throughout the brain and spinal chord, including in the SVZ and are as numerous as neurons in the CNS (Lawson et al., 1990, Lawson et al., 1992). The microglia have their developmental origin from yolk-sac macrophages, and invade the brain before vascularization occurs. Microglia are considered mononuclear cells distinct from immune cells of the hematopoietic system, but are functionally similar and share expression of many of the same surface markers (van Furth et al., 1972, Murray and Wynn, 2011). When activated, microglia become phagocytic, highly migratory, and are attracted to sites of injury primarily by inflammatory cytokine signaling. Activation can occur through several different paths. Classically activated macrophages (M1) respond to pathogens like virus and bacteria. Alternatively activated macrophages (M2) are important in wound healing and have anti-inflammatory properties (Murray and Wynn, 2011). Additionally, a specific subset of macrophages can be found in tumors. These tumor-associated macrophages (TAMs) have been suggested to be involved in both tumor progression and recession (Bingle et al., 2002). Microglia are important modulators of neurogenesis both in the hippocampus and SVZ, secreting factors like BDNF and TGF-α (transforming growth factor beta) stimulating proliferation and neural differentiation (Walton et al., 2006, Liao et al., 2008). In the hippocampus, microglia and T-cells support neurogenesis and are implicated in hippocampal functions related to learning and memory (Ziv et al., 2006). Regional differences of the neurogenic niches in response to ionizing irradiation (Hellstrom et al., 2009) could be attributed to distinct populations of microglia populating the two main neurogenic zones of the brain. We demonstrated differences in the expressions of growth factors, like fibroblast growth factor-2 (FGF2) and leukemia inhibitory factor (LIF) in microglia sorted by FACS. These growth factors stimulated proliferation and reduced cell death in neurosphere cultures (Hellstrom et al., 2011).

Molecular control of adult neurogenesis

Neural stem cell behavior, in terms of proliferation, fate determination, and differentiation is to a great extent controlled by the expression of transcription factors. Transcription factors bind to DNA and regulate gene expression by either

activating or repressing mRNA transcription. Transcription factors important for controlling neural stem cell behavior are the bHLH (basic helix-loop-helix) transcription factors, which regulate both neurogenesis and oligodendrogenesis (Yun et al., 2002, Roybon et al., 2009). Forced expression of pro-neural bHLH transcription factors Mash1, neuroD and neurogenin can cause multipotent P19 carcinoma cells to differentiate into neurons (Farah et al., 2000). In Neurogenin2 and Mash1 double mutant mice cortical progenitors fail to differentiate into neurons and remain pluripotent or choose a glial fate (Nieto et al., 2001). In the adult brain, Mash1 (also known as Ascl1) is expressed by C-cells, neuroblasts, and oligodendrocyte progenitor cells (OPCs). Mash1 knockout mice die soon after birth and exhibit a substantially smaller olfactory bulb containing fewer neural progenitor cells and OPCs. Mutant cells transplanted into the wildtype brain still fail to generate neurons and oligodendrocytes, in contrast to wildtype cells transplanted into the mutant brain, indicating a strictly intrinsic role of Mash1 in neuronal and oligodendrocytic fate determination (Parras et al., 2004). Another bHLH transcription factor involved in SVZ oligodendrogenesis is Olig2. Much like Mash1, Olig2 is expressed by C-cells and OPCs, but not by neuroblasts. Overexpressing Olig2 in the SVZ leads to increased oligodendrogenesis at the expense of neurogenesis, and inhibition results in abolished oligodendrogenesis (Hack et al., 2005).

An integral step in the DNA-binding process of bHLH factors is heterodimerization with enhancer motifs on E proteins E12 and E47 (Murre et al., 1989). By binding competitively to E12 and E47 inhibitor of DNA binding (Id) proteins can prevent the function of bHLH transcription factors. Id genes are expressed extensively in the developing CNS by neuroepithelial cells and neuroblasts, but also by astrocytes and microglia (Neuman et al., 1993, Jen et al., 1997, Andres-Barquin et al., 1998, Tzeng et al., 1999, Tzeng, 2003). Interestingly, Id1 is highly expressed in B-cells and thought to be involved in self-renewal capacity, while Id2 and Id4 regulate oligodendrocyte lineage-commitment in neural stem cells (Samanta and Kessler, 2004, Nam and Benezra, 2009).

Gene expression in neural stem cells is also regulated by soluble and membrane-bound factors, which play a significant role in neural stem cell proliferation, survival, and differentiation. The Wnt signaling pathway regulates

both SVZ proliferation and neuronal differentiation. Binding of Wnt to its receptor Frizzled prevents beta-catenin degradation by GSK3-β, allowing β-catenin to translocate into the nucleus and activate gene expression (Cadigan and Nusse, 1997). In the SVZ, β-catenin is expressed by B- and C-cells and overexpression results in increased proliferation and inhibited differentiation of Mash1-expressing progenitors (Adachi et al., 2007). Another prominent signaling pathway important in the regulation of adult neurogenesis is the notch pathway. Notch signaling is activated when the notch receptor binds to membrane-bound ligands Jagged and Delta on neighboring cells. This causes enzymatic cleavage of the notch intracellular domain (NICD) by gamma-secretase. NCID binds to RBPj and induces gene expression (Hori et al., 2013). Notch signaling (notch1) in SVZ adult neurogenesis is suggested to be involved in maintaining the regenerative ability of mitotically active B-cells. Selective conditional deletion of notch1 in nestin expressing stem cells (B-cells) did not reduce the number of B-cells, however it reduced the number of neuroblasts generated after anti-mitotic AraC (arabinofuranosyl cytidine) treatment. Moreover, quiescent B-cells were continuously lost over time and were significantly reduced in aged animals following AraC treatment. Notch1 could therefore be important for maintaining an activated proliferative subset of B-cells, which is distinct from the quiescent B-cells. Anti-mitotic treatment and aging, in the absence of notch1, putatively draws from the limited number of quiescent cells, instead of the activated B-cells, to fuel neurogenesis, leading to an accelerated decline in neurogenesis (Basak et al., 2012).

Epidermal growth factor

EGF was originally discovered by Stanley Cohen (Cohen, 1962). He treated newborn mice with extracts from the submaxillary salivary gland causing premature opening of eyelids and exposure of teeth. The discovery was made in the wake of Cohen's and Rita Levi-Montalcini's discovery of the first neurotrophic factor, nerve growth factor (NGF) (Cohen and Levi-Montalcini, 1957). In an attempt to identify the active agent in the tumor extract, that we now know was NGF, Cohen added phosphodiesterase to the extract in order to destroy all nucleic acids. The phosphodiesterase was derived from snake venom, and

to Cohen's surprise he found extensive nerve outgrowth in the control cultures only containing phosphodiesterase. Amazingly, the stimulatory effect was completely abolished by adding snake venom antidote to the cultures (Cohen, 1959), indicating that the snake-derived phosphodiesterase contained a growth factor distinct from NGF. Cohen subsequently started to investigate factors in mice salivary glands and soon after identified the new growth factor and named it EGF. The name *epidermal growth factor* was given due to its mitogenic effect on chick embryo epidermal cells (Cohen, 1965). In 1986 Levi-Montalcini and Cohen shared the Nobel prize in physiology or medicine.

EGF is one of several ligands that bind to the EGF receptor (EGFR). EGFR also called ErbB1 (avian erythroblastosis oncogene B1), is a member of the ErbB receptors (ErbB1-4). The ErbB's belong to the receptor tyrosine kinase (RTK) family of transmembrane receptors. Most RTKs are monomeric, but dimerize on ligand binding. When dimerized, intracellular tyrosine residues on the receptor are phosphorylated, leading to activation of intracellular tyrosine-binding proteins (Gerbin, 2010). Activation of ErbB's can have diverse effects, which in part is due to the large number of tyrosine residues than can be phosphorylated upon ligand binding (Jones et al., 2006). ErbB receptors are involved in an abundance of cellular functions, including proliferation, apoptosis, migration, and survival (Yarden and Sliwkowski, 2001).

Of the four ErbB receptors, only ErbB1 and ErbB4 are fully functional receptors with ligand-binding domains and kinase activity. ErbB1 and ErbB4 can signal either via homodimerization or by heterodimerization with either ErbB2 or ErbB3. ErbB2 lacks a ligand-binding domain while ErbB3 has only minimal kinase activity. Both receptors depend on heterodimerization with ErbB1 or ErbB4 for signal transduction (Figure 2)(Gerbin, 2010). Different ErbB ligands bind to a distinct set of ErbB receptors. Some, like EGF and TGF-α (transforming growth factor alpha) exclusively bind to ErbB1, others like HB-EGF use both ErbB1 and ErbB4 receptors, and factors, like the neuregulins, exclusively bind to ErbB3 and ErbB4 (Yarden and Sliwkowski, 2001). Due to the extensive heterodimerization between the different ErbB´s, attributing distinct effects of specific ligands is difficult. The same is true for isolating individual intracellular pathways activated by ligand-receptor binding.

Systemic deficiency or loss of activity of ErbB signaling can lead to reduced skin wound healing, defective hair development, or female reproductive impairments (Shirakata et al., 2005, Schneider and Wolf, 2008, 2009). Of all ErbB ligands only loss of HB-EGF is fatal, leading to postnatal death due to dysfunctional heart and lungs (Iwamoto et al., 2003, Jackson et al., 2003). Overexpression of ErbB signaling frequently leads to hyperproliferation, inflammation, and tumorigenesis (Sandgren et al., 1990, Vassar and Fuchs, 1991, Cook et al., 1997).

One of the main signaling pathways activated upon EGFR activation is the Ras/MAPK pathway. Ligand binding to the EGFR leads to autophosphorlyation of tyrosine residues on the receptor intracellular domain, which allows the adaptor protein Grb2, located in the cytosol, to bind to the EGFR (Batzer et al., 1994). Grb2 is bound to the Ras exchange factor Sos. Sos activates membrane-bound Ras by exchanging Ras GDP to GTP. Ras-GTP subsequently activates the Raf-1 kinase leading to MAPK phosphorylation and nuclear translocation (Hallberg et al., 1994, Langlois et al., 1995). Downstream events following MAPK signaling include activation of transcription factors like c-Myc, CREB, and c-Fos (Jorissen et al., 2003).

Phospholipase C-γ (PLCγ) and phosphatidylinotisol-3-kinase (PI3-K) are enzymes involved in phospholipid metabolism and are both activated upon EGFR phosphorylation (Wahl et al., 1990, Chattopadhyay et al., 1999). Activated PLCγ cleaves phosphatidylinositol 4,5-bisphosphate (PIP$_2$) bound to the plasma membrane, generating diacyl glycerol (DAG) and inositol 1,4,5-triphosphate (IP$_3$). IP$_3$ triggers Ca^{2+} release leading to activation of calmodulin kinases (CaMK) and DAG serves as a cofactor for activation of protein kinase C (PKC) (Jorissen et al., 2003). Signaling through Ca^{2+} is important in cell survival, and increases in intracellular Ca^{2+} can trigger apoptosis (Berridge et al., 2000). Activation of PI3-K by the EGFR receptor can lead to formation of phosphatidylinositol 4,5-trisphosphate (PIP$_3$). Lastly, PI3-K signaling, acting through Akt/PKB (protein kinase B) is one of the most important signaling pathways in mediating proliferative and anti-apoptotic effects of EGFR activation (Jorissen et al., 2003). EGFR signaling pathways are summarized in Figure 2.
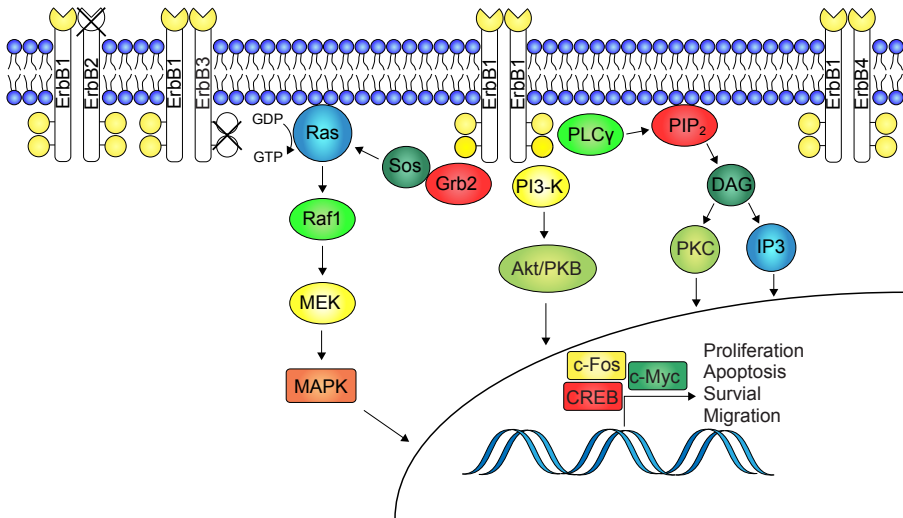
Figure 2. EGFR receptor intracellular signaling pathways and ErbB receptor hetereodimerization

Epidermal growth factor signaling in adult neurogenesis

Reynolds and Weiss (1992) performed one of the first studies demonstrating the importance of EGF-signaling on adult neural stem cells. Cells isolated from the adult mouse ventricle walls proliferate *in vitro* and give rise to both neurons and astrocytes when cultured without serum, but only in the presence of EGF. The proliferating cells form free-floating clusters, called neurospheres. In addition to EGF, a non-adhesive substrate is required for sphere formation. Interestingly, other mitogens like basic fibroblast growth factor (bFGF) and platelet-derived growth factor (PDGF) did not replicate the effects of EGF on proliferation and sphere formation. Neural stem cells express the intermediate filament protein nestin, which is also expressed by neuroepithelial stem cells in the developing CNS (Lendahl et al., 1990).

Using osmotic minipumps, Craig and colleagues, infused EGF intracerebroventricularly (ICV) in mice for six days resulting in increased proliferation and invasion of cells into the parenchyma surrounding the ventricles (Craig et al., 1996). Cells isolated from the EGF-treated ventricle wall gave rise to four times as many neurospheres *in vitro*, compared to vehicle. Lineage tracing *in vivo* using BrdU demonstrated astrocyte differentiation in favor of neuronal differentiation seven weeks after cessation of infusion. The vast majority of the

EGF-stimulated proliferative cells expressed EGFR, indicating a direct role of the exogenous EGF on the neural stem cells. Similar effects of EGF ICV infusion are present in rat. A detailed analysis of neurogenesis and gliogenesis following 14 days of EGF infusion revealed a ten-fold increase in SVZ proliferation (Kuhn et al., 1997). However, the number of newborn cells found in the olfactory bulb four weeks after cessation of infusion was less than half compared to vehicle. In addition, the percentage of newborn neurons was reduced, and the percentage of newborn astrocytes increased in EGF-treated animals. One striking difference following EGF-treatment in rats, which is not observed in mice, is the presence of hyperplastic polyps formed in the EGF-treated rat SVZ. The highly proliferative polyps are immunonegative to both neuronal and mature astrocyte markers (NeuN and S100β respectively) (Kuhn et al., 1997). The hyperproliferative polyps have been described following TGF-α infusion into the dopamine-depleted rat striatum and following EGF infusion into and the ischemic rat brain (de Chevigny et al., 2008, Sun et al., 2010). One study has described EGF-induced polyp-formation in the mouse SVZ (Ninomiya et al., 2006).

These studies demonstrated for the first time the proliferative capability and EGF responsiveness of adult SVZ neural progenitors *in vitro* and *in vivo* (Reynolds and Weiss, 1992, Craig et al., 1996, Kuhn et al., 1997). However, the importance of EGF in the SVZ lineage progression under physiological conditions was still not known. At the time, previous characterizations of the SVZ suggested the presence of a transit-amplifying proliferative cell, the C-cell (Doetsch et al., 1997). However, the characteristics were based on ultrastructural properties and no immunohistochemical markers were available to identify the C-cell. Characterization using an antibody against EGFR revealed that EGFR was predominately expressed by SVZ C-cells. Additionally, a subset of GFAP expressing astrocytes with processes contacting the ventricle expressed EGFR. Following EGF infusion for six days the percentage of proliferating C-cells increased while the number of proliferative neuroblasts decreased. Genetic lineage tracing demonstrated that few SVZ-derived neural stem cell migrated to the olfactory bulb following EGF infusion and the number PSA-NCAM expressing cells in the SVZ had diminished significantly. Instead, labeled cells were found in the striatum, corpus callosum, and cortex. Using transgenic

mice expressing thymidine kinase under the Dlx2 promoter, selectively killing C-cells, the EGF-induced proliferative response was greatly reduced, indicating that the C-cells are the EGF-responsive cells. However, after prolonged EGF-infusion for six days, Dlx2 expression was greatly reduced in the SVZ. In contrast, tenascin-C normally expressed by astrocytes and in the ECM during development, increased in the periventricular area, suggesting a glial phenotype of the EGF-expanded cells (Doetsch et al., 2002). More details on the specific cell type expanded by EGF infusion were provided by Gonzalez-Perez and colleagues (Gonzalez-Perez et al., 2009). An avian leucosis virus system for long-term fate analysis of proliferating GFAP-positive cells confirmed the invasive nature of the EGF expanded cells. Found throughout the brain, as far as 1mm from the SVZ, the cells expressed CNPase, a marker for myelinating oligodendrocytes. When EGF infusion was preceded by chemical demyelination, using lysolecithin, EGF expanded cells migrated towards the lesion and differentiated into myelinating oligodendrocytes, ameliorating the impact of the lesion (Gonzalez-Perez et al., 2009).

NG2-expressing OPCs in the SVZ and RMS of postnatal brain express EGFR and migrate in response to EGF stimulation (Aguirre et al., 2005). Interestingly, EGF-induced migration of NG2-cells required interaction with the ECM. Blocking ECM-integrin interactions inhibited EGF-induced migration of SVZ and RMS NG2 cells. These EGF-induced properties are not found in cortical NG2-expressing OPCs, but could be induced by EGFR overexpression (Aguirre et al., 2005). Selective overexpression of the human EGFR driven by the Cnp promoter expands the NG2 population in mice. Cnp is expressed by OPCs and the SVZ of Cnp-hEGFR animals display reduced B-cell number while OPC numbers are increased. The reduction in B-cells was mediated by EGFR-induced Notch inhibition through Numb, suggesting a role of EGFR and Notch in maintaining the balance of quiescent B-cells and proliferative progenitors (Aguirre et al., 2010).

Ionizing irradiation

Ionizing irradiation or γ-irradiation is electromagnetic radiation of high-energy photons. By definition ionizing irradiation has the energy to displace electrons

from atoms. This property is utilized clinically in radiation therapy to induce tissue damage and cell death when targeting tumors. The degree of damage caused is dependent on the radiation dose (Gray, Gy), the size of the irradiated area, the age of the patient and whether the irradiation is given as a single dose or fractionated over time (Packer et al., 1987). Differences in radiation sensitivity have traditionally been linked to mitotic activity and cellular maturity; implying that immature proliferative cells, like cancer cells and stem cells, are more sensitive than post-mitotic cells. This rule is called '*the law of Bergonié and Tribondeau*', named after the French physicist and physician Jean Alban Bergonié and the histologist Louis Tribondeau. Using the newly discovered X-rays to treat reproductive organs and tumors they observed that certain tumor types and healthy germinal cells were more sensitive to irradiation than the healthy surrounding tissue. This fact led them to postulate that radiosensitivity is linked to proliferative activity (republished in English by (Bergonie and Tribondeau, 1959)). These findings were revolutionary and the scientific impact should not be underestimated. However, today we know that these generalized rules are have their limit to properly explain differences in radiosensitivity in both tumor and normal cells (Vogin and Foray, 2013).

When high-energy photons enter the tissue, electrons are removed (or ionized) from molecules, resulting in structural changes. The DNA is particularly vulnerable to the removal of electrons, leading to changes in individual nucleotides or breakage of one or both of the DNA strands, called single (SSB) or double strand breaks (DSB) respectively (Figure 3A). Single strand breaks occur frequently, even in healthy cells and are repaired with high accuracy by several different mechanisms (Friedberg et al., 2004, Wilson et al., 2011, Azzam et al., 2012). Double strand breaks are harder to repair, due to the fact that information on the complementary strand might not be present, which can lead to a loss of genetic information after repair. In addition, the terminal bases on the broken strand are often damaged in the process, making ligation difficult (Jackson, 2002). Cells demonstrate different sensitivity towards ionizing irradiation depending on the cell cycle stage. During the G2 and M-phase (mitotic phase) cells are generally more susceptible to irradiation-induced damage, whereas the late S-phase is the most radioresistant part of the cell cycle. The DNA-damaging effects of ionizing irradiation itself are known as direct effects; additionally, in-

direct damage can be caused as a result of the high-energy photons reacting with other molecules such as H_2O. This leads to creation of highly reactive free radicals causing indirect oxidative damage to cells. The ionizing radiation reacting with H_2O creates mainly the reactive oxygen species (ROS) $O2^{\cdot-}$, $OH^{\cdot}$, and H_2O_2 (Azzam et al., 2012) (Figure 3A). The sensitivity of specific cell types to radiation is to a large extent determined by the ability to repair DNA damage and is regulated by the DNA damage response (DDR) pathways (Figure 3B). In the event of DNA damage, the kinases ATM (ataxia Telangiesica-Mutated), ATR (ATM/Rad3-realted), and DNA-PK (DNA-dependent protein kinase) are activated (Durocher and Jackson, 2001). DNA-PK regulates non-homologous end joining (NHEJ) DNA repair, ATM and ATR control cell cycle progression via checkpoint kinases (Chk1 and Chk2), and apoptosis via p53 (Harper and Elledge, 2007).

Recently, a new mechanism of radiation-induced cellular damage has been proposed. According to this concept cells spared from direct irradiation can still suffer irradiation induced-damage through signaling from irradiated cells. This process is called radiation-induced bystander effects (RIBE) (Nagasawa and Little, 1992). Reported RIBEs include changes in gene expression, genomic instability, and cell death (Sjostedt and Bezak, 2010). Small molecules like ROS, NO, and Ca^{2+} can influence nearby cells via gap junctions and soluble factors like TGF-α and cytochrome-c (Narayanan et al., 1997, Shao et al., 2008, He et al., 2011). Another clue to the mechanisms behind radiosensitivity comes from research on ceramide. Apoptotic stimuli, such as death receptor activation, can lead to de novo synthesis of ceramide, which promotes cleavage and activation of caspases, thereby causing caspase-dependent cell death (Dhein et al., 1995, Monney et al., 1998, Lin et al., 2006). In addition, ceramide can be produced through hydrolysis of sphingomyelin in the plasma membrane. Sphingomyelin is a sphingolipid enriched in plasma membrane lipid rafts. Lipid rafts are thought to function as signaling platforms by aggregating receptors, like EGFR (Balbis et al., 2007, Bieberich, 2012). Sphingolipids are highly expressed by neural stem cell and cancer cells, and inhibition of sphingolipid metabolism in neuroepithelial cells disrupts neural tube development (Marasas et al., 2004, Li et al., 2006, Patra, 2008). The enzyme responsible for ceramide release through sphingomyelin hydrolysis is acid sphingomyelinase (ASM). Membrane-bound

ASM can be activated by ionizing irradiation and trigger apoptosis (Figure 3A). Moreover, cancer cells deficient in ASM show reduced irradiation-induced apoptosis (Santana et al., 1996).
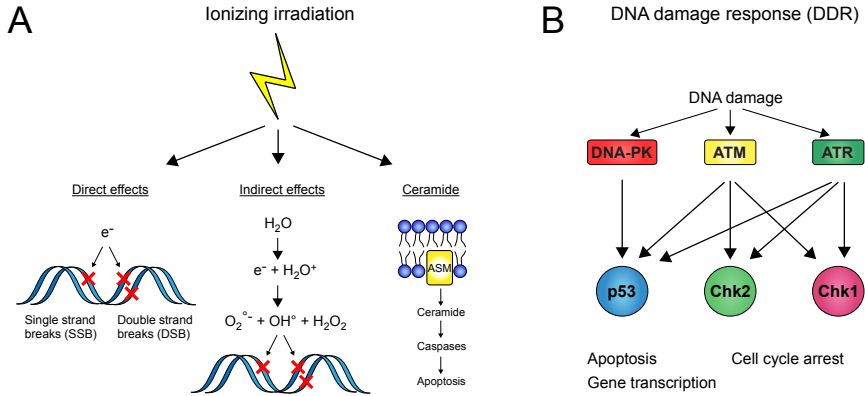
Figure 3. (A) Direct and indirect cellular responses to irradiation. Activation of acid sphingomyelinase (ASM) can result in ceramide-induced apoptosis. (B) Direct and indirect effects lead to activation of the DNA damage response

Neural stem cells and irradiation

In the adult brain the stem cell populations of the SVZ and the hippocampus are severely affected by ionizing irradiation in a dose dependent manner. Following irradiation, the total cell number and neural progenitor cell number is rapidly reduced (Hubbard and Hopewell, 1980). However, the rapid drop in proliferation immediately after irradiation is followed by a transient increase in proliferation, which occurs for as long as seven days, only to gradually decrease thereafter. The extent of the transient increase and the resulting baseline level of proliferation are inversely related to the irradiation dose (Tada et al., 1999). Age is a strong determining factor on the negative effects of irradiation on the brain as a whole, but also specifically on neurogenesis (Packer et al., 1987). Comparing the postnatal rat brain (postnatal day 9) to the juvenile rat brain (postnatal day 23), irradiation-induced damage, in terms of cell loss, is greater in the postnatal brain (Fukuda et al., 2005). Moreover, postnatal irradiation has differential effects on the stem cell niches of the brain. Nine weeks following 6 Gy-irradiation at P9 the SVZ exhibited proliferation at 50% of the control, whereas the proliferation in the irradiated hippocampus was only 5%

of the control (Hellstrom et al., 2009). In the SVZ the majority of the cell loss, both acute and long-term, following irradiation is attributed to loss of transit-amplifying C-cells and neuroblasts. The quiescent stem cells (B-cells) appear to be more resistant to irradiation-induced cell death (Achanta et al., 2012, Pineda et al., 2013). In contrast to treatment using anti-mitotic drugs, the stem and progenitor cells of the irradiated SVZ does not fully recover (Doetsch et al., 1999b, Doetsch et al., 2002, Pineda et al., 2013). Moreover, naïve stem cells, transplanted into an irradiated neurogenic niche, fail to proliferate, and irradiated neural stem cells can be induced to proliferate if cultured *in vitro* (Monje et al., 2002, Pineda et al., 2013). These results suggest that extrinsic factors in the irradiated SVZ are, at least in part, responsible for the anti-neurogenic effects of irradiation. In the SVZ, endothelial cells secrete TGF-β1 as a result of irradiation. TGF-β1 acts as a suppressor of neurogenesis, and the negative effects of irradiation on neurogenesis can be ameliorated by blocking TGF-β1 signaling (Pineda et al., 2013).

MATERIAL AND METHODS

Animals

All experiments were approved by the Gothenburg Committee of the Swedish Animal Welfare Agency (application nos. 214-07, 145-10, and 154/12). Male Fischer-344 or Wistar rats (Charles River, Germany) were used and housed in a barrier facility with ad libitum access to food and water with a 12-h light/dark cycle. In Paper IV the animals were delivered to the animal housing facility at postnatal day 8 in litters of ten with each dam.

Comments:

In the current thesis animals from an age of postnatal day 9 (P9) to ~3 months of age were used. When studying adult neurogenesis animals considered as young adult are often used. Generally animals are considered young adult after having reached sexual maturity at around 5-6 weeks of age. SVZ neurogenesis rapidly declines during the first postnatal weeks followed by stable levels until the animals are considered aged (generally 1.5 to 2 years old), when neurogenesis declines further. In the papers included in the current thesis only male rats were used. The main reasons being that the original experiments (Kuhn et al., 1997) were performed in males. While one ideally would include male and females, initial studies focused on a single sex generally allow the use of fewer animals, due to a more homogenous experimental population. However, this potentially reduces the general applicability of the final results.

Intracerebroventricular infusion

Animals receiving growth factor treatment at P21 were anesthetized using 5% isofluorane in air and oxygen (1:1 ratio). The heads of the animals were fixed in a stereotaxic instrument with a nose cone supplying isofluorane. A skin cut was made on along the midline of the head to expose the scull. A hole for the infusion cannula was drilled at -0,4mm anterioposterior and -0,8mm mediolateral relative to bregma, using a 0,9mm diameter drill bit (Meisinger, Germany). Before placing the cannula, the osmotic minipump (Model 1002, Alzet, USA)

was placed subcutaneously on the back of the animal. The infusion cannula (Infusion kit 1, Alzet, USA) was fixed using Loctite super glue (Loctite, Ireland) and the surgery wound was closed using wound clips.

The animals receiving growth factor treatment in adulthood were anesthetized by a cocktail consisting of Ketamin (25mg/ml), 2/3 in volume and Rompun (1,27 mg/ml), 1/3 in volume administered intraperitoneally at a dose of 3 ml/kg. In order to facilitate the surgery the heads of the animals were shaved before being mounted into a stereotactic frame. The stereotactic coordinates used for cannula placement were the same as previously described (Kuhn et al., 1997): anteroposterior [AP] + 8.5mm, lateral + 1.2mm from the center of the interaural line at flat skull position; cannula length, 5mm below skull. The stainless steel cannula was inserted into the lateral ventricle after an entry site was made in the cranium using a 0,9mm diameter drill bit (Meisinger, Germany). Using dental cement and 1/16-inch-diameter screws (Plastic One, Roanoke, USA) the cannula was fixed to the skull and the pump (Model 1002, Alzet, USA) placed in a subcutaneous pocket on the animal's back. The skin cut was closed using wound clips. EGF or vehicle was infused for 1, 7, or 14 days at a dose of 360ng/day. Minipumps were filled with 30 mg/mL human recombinant EGF (Invitrogen, Carlsbad, USA) dissolved in artificial cerebrospinal fluid (aCSF) containing 100mg/mL rat serum albumin (Sigma-Aldrich, St. Louis, USA). The minipumps were primed by incubation in sterile PBS at 37°C for 24 h, to ensure no lag time in delivery after implantation. aCSF consisted of NaCl (148mM), KCl (3mM), $CaCl_2 \times 2H_2O$ (1.4mM), $MgCl_2 \times 6H_2O$ (0.8mM), Na_2HPO_4 (1.5mM), and $NaH_2PO_4 \times H_2O$ (0.2mM).

At the end of the growth factor infusion period, animals were sacrificed by overdose of pentobarbital administered intraperitoneally, followed by transcardial perfusion using 0.9% saline solution followed by phosphate-buffered (0.1 M, pH 7.4) 4% paraformaldehyde (PFA) (Thermo Fisher Scientific, Waltham, USA). Following perfusion, brains were removed and postfixed in 4% PFA for 24 hours and prepared for cryosectioning by incubation in phosphate-buffered (0.1 M pH 7.4) 30% sucrose for at least 3 days. Brains used for cellular quantification were cryosectioned coronally at a thickness of 40μm (Paper I-IV). Brains used for RMS composition analysis in Paper III were sectioned sagittaly at

25µm thickness and P21 animals in Paper IV coronally at a thickness of 25µm (Paper IV). All brains were cut using a sliding microtome (Leica Microsystems, Germany) and collected as serial sections (1 in 12 series with 480 µm distance between sections for 40µm sections and 300µm distance for 25µm sections). Sections were stored at 4˚C in a cryoprotective solution (glycerol, ethylene glycol, and 0.1 M phosphate buffer pH 7.4, 3:3:4 by volume).

Comments:

Osmotic minipumps are passive pumps that expel its content by absorbing fluid from the surrounding tissue shrinking the delivery compartment at a specific and continuous rate. Osmotic minipumps provide a good alternative to multiple individual injections performed over time, as each injection can be a stressful event for the animal. By using an ICV infusion cannula the substance can be delivered directly to the brain, without it having to pass the blood brain barrier. It also avoids possible systemic effects that might occur from peripheral delivery. The location of the SVZ, being in close vicinity of the ventricular space, ensures full exposure in the ipsilateral hemisphere, while still often giving a full to partial effect on the contralateral side, depending on the concentration. Since the ventricular system passes through the spinal chord and extends to the submeningeal compartment, the entire CNS can be expected to be exposed to the delivered substance during multi-day infusions.

Irradiation

Irradiation treatment was carried out at Jubileumskliniken at the Sahlgrenska University Hospital in Gothenburg. For irradiation a linear accelerator (Varian Clinac 600CD) with 4 MV nominal photon energy and a dose rate of 2.3Gy/minute was used.

All animals were anesthetized using tribromoethanol (Avertin, Sigma-Aldrich) that was administered intraperitoneally. Following anesthesia the animals were placed in a prone position in a polystyrene bed and were irradiated with a single dose of 8Gy. The whole brain, including the olfactory bulbs, was irradiated with a radiation field of 2 x 2 cm. The source to skin distance was approximately 99.5 cm. A 1cm thick piece of tissue-equivalent material was put over the animals

to ensure an even irradiation dose throughout the brain. After irradiation, the pups were returned to the dams until weaning at P21. The sham-irradiated control animals were anesthetized but not subjected to irradiation, and otherwise treated identically.

For each time point (P21 and P80) four groups were included; irradiated animals which received EGF treatment (EGF Irr), irradiated animals which received aCSF (aCSF Irr), non-irradiated EGF-treated animals (EGF Sham) and non-irradiated animals which received aCSF (aCSF Sham).

Comments:

The radiation dose used can be considered moderate. Previous studies from our laboratory using 6 Gy of irradiation (Hellstrom et al., 2009) resulted in a 50% reduction in SVZ proliferation 9 weeks after postnatal day 9 irradiation. In Paper IV we aimed at a severe, but not complete reduction of SVZ proliferation and therefore used a dose of 8 Gy. The impact of irradiation is also highly influenced by age (Fukuda et al., 2005), being more severe in younger individuals. Although it is difficult to designate a human equivalent to the age when irradiation was given, a cautious estimate is perinatal or early postnatal. Additionally, it is difficult to establish an equivalent dose in a clinical setting. We employed a paradigm where a single dose was used, while clinically radiation therapy is generally administered in fractionated doses. In Paper IV only the SVZ was studied, however the entire brain received irradiation, potentially leading to other changes influencing neurogenesis.

Immunofluorescence

The sections were washed 3 times in Tris-buffered saline (TBS) followed by blocking for 1h in TBS, 3% normal donkey serum (Jackson ImmunoResearch, West Grove, USA), and 0.1% Triton-X at room temperature. For immunostaining against phospho-histone H3 (pHH3), an antigen retrieval step in sodium citrate (pH 6) at 80°C for 20min was employed. For all immunostainings where rabbit anti-radixin or mouse anti-radixin were used, the initial washing step was followed by antigen retrieval in sodium citrate pH6 at 97°C for 20 minutes. Sections used for BrdU immunofluorescence were treated with 2M

HCl for 30 minutes at room temperature or 37°C followed by neutralization in 0.1M borate buffer. Primary antibodies were diluted in blocking solution and sections were incubated for 24–72h at 4°C. For primary antibodies used, see Table 1. Sections were then washed 3 times in TBS and incubated with secondary antibodies: donkey (Dk) anti-goat 488 IgG, Dk anti-goat 546 IgG, Dk anti-mouse 488 IgG, Dk anti-mouse 555 IgG, Dk anti-mouse 647 IgG, Dk anti-rabbit 488 IgG, Dk anti-rat 488 IgG (1:2,000, Alexa Fluor; Molecular Probes, Eugene, USA), Dk anti-chicken FITC IgG (1:2,000, Jackson ImmunoResearch), and Dk anti-rabbit IgG CF568, Dk anti-rabbit IgG CF555, Dk anti-goat IgG CF555, Dk anti-goat IgG CF633, Dk anti-mouse IgG CF488 (1:1,000; Biotium, Hayward, USA).

ToPro3 or YoPro1 were used as nuclear stains (Molecular Probes). Secondary antibody incubation was performed for 2h at room temperature, followed by 5 rinses in TBS. The sections were mounted on slides and coverslipped with ProLong Gold (Molecular Probes/Invitrogen, Carlsbad, USA).

Comments:

Immunofluorescence is a flexible method to detect the distribution of protein expression of single or multiple proteins simultaneously. Final results will vary depending of fixation, primary and secondary antibody concentrations, pre-treatments, age and species of the tissue, making the method ill suited for studying absolute protein levels. Tissue pre-treatments, using heat, acids, or solvents, can help reveal the target epitope to the primary antibody, but also change the structure of other epitopes reducing the binding of other antibodies. To ensure high specificity, well-characterized primary and secondary antibodies were used and occasionally several antibodies against the same protein. Incubation of antibodies at lower temperature over longer period of time was employed to reduce unspecific binding of the antibodies.

Proliferation

In Paper I and IV, analysis of the proliferating population in the SVZ was performed using the M-phase marker pHH3. In project I the percentage of mitotic cells labeled by pHH3 that were also positive for either Sox2 or Olig2

Antibody	Used to label	Host species	Company	Concentration
ßIII-tubulin	Neuroblast, neural precursor cell	Mouse	Sigma	1:1000
BrdU	Proliferating cells	Rat	Serotech	1:500
CD68 (rat)	Activated microglia	Mouse	Millipore	1:1000
CNPase	Oligodendrocyte progenitor cells (OPCs)	Mouse	Abcam	1:100
Doublecortin (DCX)	Neuroblasts	Goat	Santa Cruz	1:250, 1:500
GFAP	Astrocytes	Rabbit	Dako	1:1000
Iba1	Microglia	Rabbit	Wako	1:1000
Iba1		Goat	Wako	1:1000
Nestin (rat)	Neural stem/progenitor cells	Mouse	BD Pharmigen	1:500
NG2	OPCs/Pericytes	Mouse	Millipore	1:500
NG2		Rabbit	Millipore	1:500
Olig2	OPCs, progenitor cell	Goat	R&D Systems	1:500, 1:1000
pERM	Activated ERM	Rabbit	Cell Signaling	1:500
pHH3	Mitotic cells	Rabbit	Millipore	1:1000
Radixin	Neuroblasts/OPCs	Mouse	Abnova	1:250
Radixin		Rabbit	Abcam	1:250
RECA-1	Endothelial cells	Mouse	Monosan	1:300
Sox2	Neural stem cells/radial glia	Rabbit	Millipore	1:500
Sox2		Goat	Santa Cruz	1:250
Vimentin	Astrocytes	Chicken	Millipore	1:200

Table 1. Primary antibodies used for immunofluorescence

was determined using confocal microscopy.

In project III proliferation was studied using BrdU, injected three times during the last 24 hours of EGF or vehicle infusion. BrdU/radixin and BrdU/Olig2 colabeling were analyzed by selecting at least 250 BrdU positive cells in the RMS per animal for colocalization of immunosignals. $Sox2^{high/low}$ expression in the expanded Olig2 population of the EGF-treated RMS was quantified at 3 to 4 locations in a total of about 75 $Olig2^+$ cells per animal after 7 days of EGF infusion.

Comments:

Proliferation is mainly visualized by two methods. By endogenous protein expression of cell cycle-regulated proteins or by injecting nucleotide analogs to detect DNA synthesis at specific times. BrdU, IdU, CldU (bromo-, iodo, chlorodeoxyuridine) are examples of nucleotide analogs that are inserted into the DNA during the S-phase instead of thymidine. By timing the injections of the nucleotide analogs one can label specific cohorts of cells and study different aspects of neurogenesis, such as survival and label retention. The artificial bases can later be detected with high specificity by antibody due to the fact that

they are not naturally occurring in the brain. However, their detection by immunohistochemistry requires harsh HCl pretreatment to expose the DNA to antibody detection. This can alter the structure of other proteins, occasionally complicating coexpression analyses.

Apoptosis

For analysis of apoptosis ApopTag Fluorescein Direct in situ apoptosis detection kit (Millipore) was used. Sections were mounted on Superfrost Plus microscope slides (Thermo Scientific, USA) and dehydrated in increasing concentrations of ethanol (70-99,5%), followed by a quick submersion in xylene, rehydration and wash in TBS. The sections were subsequently post-fixed in 70% ethanol and acetic acid mixed 2:1 at -20°C for 5 minutes. To allow proper designation of polyp stage, microglial cells were labeled using a rabbit anti-Iba1 primary antibody. Following 30 minutes of blocking, the sections were incubated with rabbit anti-Iba1 (1:100, Wako) for 30 minutes at 37°C. After washing in TBS sections were incubated with a dk anti-rabbit Alexa 555 secondary antibody and ToPro3 nuclear dye for 30 minutes at 37°C. followed by washing. Apoptotic cells were labeled according to the instructions of the manufacturer.

Comments:

ApopTag uses terminal deoxynucleotidyl transferase dUTP nick end labeling (TUNEL) technology to detect fragmented DNA (Gavrieli et al., 1992). Apoptosis is a multi-step process where DNA fragmentation occurs at the later stages. The method was originally developed for PFA fixed paraffin embedded tissue and cells. Certain optimization is required for its successful application on free-floating sections, like dehydration - xylene immersion - rehydration, and ethanol/acetic acid treatment.

Morphological analysis and quantification

In Paper I and IV the SVZ was visualized by DAPI (4,6-diamidino-2- phenyl-indole, dihydrochloride, ProLong Gold with DAPI; Molecular Probes/Invitrogen) and the area was measured on at least 3 sections per animal, representing

1/12th of the structure, between anterioposterior coordinates 10.3 and 7.2mm from interaural line for volume extrapolation (Paxinos and Watson, 2005). The contralateral SVZ volume was calculated using a Leica DM6000 B microscope (Leica Microsystems, Germany) and StereoInvestigator 8 software (MBF Bioscience, Williston, USA). In Paper I immunofluorescence for cell-specific protein expression was analyzed using a Leica SP2 scanning confocal microscope (Leica Microsystems). About 100–300 cells per animal were randomly selected in the contralateral SVZ of control and EGF-treated animals using ToPro3 (Molecular Probes/ Invitrogen), along with 100 cells per contralateral hyperplastic polyp. The contralateral SVZ was analyzed to avoid possible artifacts due to tissue damages from the cannula. Analysis was performed on confocal image stacks with combined thickness 6–7 μm acquired at 1.5 μm increments. For all quantifications in Paper III, coronal sections were used. Immunofluorescence was visualized using a Leica SP2 scanning confocal microscope and a 63x objective. Each fluorochrome was recorded individually in sequential scan mode to avoid channel mixing. Images were acquired from the RMS (anterioposterior coordinates 11.35 mm to 14.50 mm from interaural line (Paxinos and Watson, 2005)) in z-stacks of 2 μm increments. For radixin/DCX and radixin/Olig2 quantifications, cell nuclei were selected at random in the RMS, using ToPro3 and analyzed for either single or double immunoreactivity.

In project IV, dorsal SVZ and polyp cellular compositions were calculated by analyzing antibody expression in randomly selected cells using the nuclear dye ToPro3 (Molecular Probes, USA) from 5 confocal images acquired at 1μm intervals with a 63x objective. For all cellular quantifications double labeling was assumed when cells exhibited direct colocalization or when nucleus and cytosol or processes from the same cell were individually labeled. Quantification of confocal microscopy images was performed in ImageJ (http://rsb. info. nih. gov/ij/) using the LOCI plugin. The image stacks used for figures were processed in ImageJ and arranged in Adobe Photoshop CS5 and Adobe Illustrator CS5 (Adobe systems).

Comments:

In the current thesis, in vivo and in vitro quantifications were performed using both epifluorescence and confocal microscopy. Using epifluoresence and stereological principles, extensive quantification of structure volume, cellular density, and labeling index can be readily performed by systematic subsampling and extrapolation. One of the major drawbacks of epifluoresence is the lack of depth resolution along the Z-axis. As the entire thickness of the sample is illuminated, the position of a cell in the Z-plane is difficult to establish. This can be partially overcome using thinner tissue sections, for example when embedding tissue in paraffin. A thickness of ~5μm can then be employed instead of 25-40μm used for free-floating sections. Alternatively, confocal laser microscopy allows the generation of thin optical sections within thick tissue sections. Using lasers to excite fluorophores at specific wavelengths and a pinhole to regulate the depth of the focal plane, the accuracy of analyzing coexpression of proteins labeled by immunofluorescence is greatly improved. The main drawback of using confocal microscopy to quantify cellular changes is the inherent slowness of the scanning process to acquire images, insufficient means to quantify during image acquisition, and the fact that the high magnification required for cellular analysis is not practical when analyzing large structures.

Transmission electron microscopy

In Paper I, animals used for electron microscopy were perfused as using 4% PFA and in Paper II using 2% PFA and 0,2% glutaraldehyde. The brains were postfixed overnight in a modified Karnowsky's solution (2% PFA, 2.5% glutaraldehyde, and 0.05% Na-azide in 0.05M Na-cacodylate). The tissue used for Paper II was sectioned at a thickness of 50 μm using a Leica VT1000S vibratome (Leica Microsystems). All tissue was subsequently incubated in 1% OsO_4 (osmium tetroxide) and 1% $K_4Fe(CN)6$ (potassium ferrocyanide) in 0.1M Na-cacodylate for 2h. Following treatment with uranylacetate, the tissue was dehydrated using a graded series of ethanol and then infiltrated using acetone and Agar 100 resin (Agar 100; Agar Scientific Ltd., Stanstead, United Kingdom). After evaluation of semithin sections (0.5mm), 60–70-nm sections were cut using a Reichert-Jung Ultracut E (Leica Microsystems). Sections were counter-

stained using lead citrate and uranylacetate and collected on copper grids. The sections were imaged using a LEO912AB transmission electron microscope (Zeiss, Oberkochen, Germany) equipped with a Megaview III CCD camera (Olympus Soft Imaging Solutions, Hamburg, Germany).

Comments:

Electron microscopy is still unsurpassed when it comes to high-resolution microscopy. The reliance on electrons instead of visible light allows visualization of objects in the low-nanometer range. Transmission electron microscopy (TEM) is most frequently used for morphological studies, where the tissue is treated with contrast agents in the form of heavy metals to improve the signal. However, morphological analysis can be combined with immunohistochemistry using secondary antibodies with conjugated gold particles of discrete sizes, or by using biotinylated secondary antibodies to drive diaminobenzidine (DAB) deposition. The quality of the acquired images is to a great extent determined by the quality of fixation, tissue processing, and sectioning. The area of the sections that can be analyzed is only a few mm^2 and the thickness 50-70nm makes analysis or reconstruction of larger structures extremely time consuming.

Scanning electron microscopy

For scanning electron microscopy (SEM), the ipsilateral SVZ was dissected after perfusion and postfixed in modified Karnowsky's solution. After rinsing the tissue with sodium cacodylate buffer, the tissue was made conductive by repeated treatment with OsO_4 (Reiss, 1992). The tissue was then dehydrated in a graded series of ethanol and dried using hexamethyldizilasane. When mounted, the tissue was sputtered with palladium and examined using a Zeiss DSM 982 Gemini scanning electron microscope (Zeiss).

SVZ explant cultures

Animals were anesthetized using isofluorane and decapitated. The brains were dissected and placed in ice cold HBBS (Hank's balanced salt solution) until further processing. One-millimeter coronal slices were cut between anterio-

posterior coordinates bregma 20.5–2.5 using a coronal brain matrix. The slices were kept on ice while the lateral ventricle walls were removed and cut into 50–200 mm diameter pieces. The tissue pieces were resuspended in Neurobasal A medium (Invitrogen) and mixed 1:3 with Matrigel (BD Bioscience). 15 ml of the Matrigel-tissue mixture was dispensed in 8-well chamber slides (BD Bioscience), followed by 10 minutes polymerization at 37°C. Explants were grown in Neurobasal A medium, supplemented with B27 and Glutamax, PenStrep (All from Invitrogen). The explants cultures were kept at 37°C in 5% O_2 and 1% CO_2 for 72 h. At the end of the experiment the explants were fixed in 4% PFA for 20 minutes. Immunocytochemistry was performed in chamber slides. Following three 15-minute washes in PBS unspecific antibody binding was blocked by incubation with 3% donkey serum and 0.2% Triton-X in PBS for three hours at room temperature. Explants were then incubated with primary antibodies (see Table 1) for 72 h at 4°C, followed by three 15-minute washes in PBS and secondary antibody incubation for 2 hours at room temperature. After additional washing steps, the explant cultures were coverslipped using Prolong Gold with DAPI (Molecular Probes) and analyzed by confocal microscopy.

Comments:

Explant cultures preserve the "niche-component" of the SVZ and allows studying migration in an in vitro-setting. This facilitates analysis of different aspects of migration with possibilities to easily manipulate the system by adding chemicals or bioactive molecules to the cultures conditions. The main drawback of the explant system is the need to use artificial ECM in the form of Matrigel and the relatively low yield in migratory explants. The constituents of Matrigel, an extracellular matrix produced by a tumor cell line, are not disclosed and could act as a confounding factor under certain conditions affecting the end result.

Gene expression analysis

For mRNA expression analysis, animals were anesthetized using isofluorane (Merck, Whitehouse Station, USA) and sacrificed by cervical decapitation. The ipsi- and contralateral SVZ of aCSF- and EGF-infused animals was microdissected and flash-frozen in liquid nitrogen (n = 5 for both groups). After ho-

mogenizing the tissue in trizol (Qiazol; Qiagen, Hilden, Germany), the mRNA was precipitated using chloroform (Merck) and then extracted using RNeasy mini or micro kits (Qiagen), depending on the sample size. The concentration and quality of the mRNA was measured using a Nanodrop ND-1000 spectrophotometer (Thermo Fisher Scientific) followed by cDNA synthesis using random hexamer primers (High-Capacity cDNA Reverse Transcription kit; Applied Biosystems, Foster City, USA). The purity of the mRNA was estimated using the Nanodrop 260/280nm ratio. Two micrograms of total RNA were synthesized into cDNA and 8ng cDNA was loaded to each 20μl qPCR reaction. Non-template controls (reactions lacking cDNA) and -RT controls (mock cDNA synthesis performed without reverse transcriptase) were included to ensure that no contamination or genomic DNA was present. For Paper I Quantitect primer assays (Qiagen) for b-actin (*Actb* QT00193473), inhibitor of DNA binding 1 (*Id1* QT00374220), inhibitor of DNA binding 2 (*Id2* QT00367640), inhibitor of DNA binding 4 (*Id4* QT00383929), EGFR (*Egfr* QT00189707), and glyceraldehyde-3-phosphate dehydrogenase (*Gapdh* QT00199633) were used according to the primer manufacturer's instructions. For Paper III primer sequences were generated using NCBI primer-BLAST (http:// www.ncbi.nlm. nih.gov/tools/primer-blast/) and Primer express software (Applied Biosystems) and synthesized by Eurofins MWG Operon (Ebersberg, Germany). Primer sequences were designed with a melting temperature of 60°C (55°C for radixin) spanning introns when possible and the efficiency of all primers was tested using a dilution curve.

Sequences used:

AAAGCCCAGGCCCAATGCGC (*Dcx*, forward)

ACAAGTCCTTGTGCTTCCGCAGAC (*Dcx*, reverse)

TGTGATGGACTCCGGAGACGGG (*Actb*, forward)

TGTAGCCACGCTCGGTCAGGAT (*Actb*, reverse)

AACCCATCACCATCTTCCAGGAGCG (*Gapdh*, forward)

ACATACTCAGCACCAGCATCACCCC (*Gapdh*, reverse)

CCTACCACAGCGTGTTTTGGA (*Radixin* forward)

TCCCCCTGTGTTCTTCATGC (*Radixin* reverse)

For self-generated primers we used an initial cycle of 15 min at 95°C, followed by repeated cycles of 94, 60/55, and 72°C (40 cycles in total). All primers were used together with Maxima SYBR green master mix (Fermentas, Burlington, Ontario, Canada). A Roche Lightcycler 480 (Roche, Basel, Switzerland) was used for PCR amplification. The efficiency of each primer was determined using a 1:4 dilution standard curve and taken into account when calculating the relative expression level. Calculations of Cq values were made in LightCycler 480 software version 1.5 (Roche). The final fold changes were calculated after correction for efficiency and normalization against 2 reference genes (*Gapdh* and *Actb*) using Cq values and the ΔΔCq method (Vandesompele et al., 2002).

Comments:

The employed method of gene expression analysis compares the relative expression of the target gene. A primer pair is used to amplify the mRNA of the gene of interest. Temperature is used to control the binding of the primer to the target region on the cDNA, the synthesis of a complementary strand, and the detachment of the primer. After binding, ligation, and synthesis the primer detaches, completing a cycle. By using a fluorescent dye that binds to double stranded DNA, the amount of amplified material can be measured over time, and the expression level is determined by the number of cycles required to reach a stage of exponential expansion. A reference gene is used to normalize the expression level. Moreover, equal amounts of mRNA are synthesized to cDNA and equal amounts of cDNA are added to each reaction. Gapdh and Actb are frequently used as reference genes, but occasionally the treatment used changes the expression of these genes. It is therefore instrumental to always control the expression of the chosen reference genes to make sure the expression stays constant. Genes chosen as reference genes only need to meet this criterion to be suitable.

Statistics

When comparing more than two groups 1-way analysis of variance was used in conjunction with Tukey's post hoc test. When comparing two groups, Student's t-test was employed, or the Mann-Whitney U-test, if the data was not considered normally distributed. Body weights in Paper IV were analyzed by multiple t-tests using Holm-Sidak correction for multiple comparison. Statistical analyses were performed in GraphPad Prism (version 4-6, GraphPad Software). Cell numbers are presented as mean±SD and percentages as mean±SEM. Error bars represent standard error of the mean (SEM) and differences resulting in p values of p<0.05 were considered statistically significant (*).

AIMS

The aim of this thesis was to study the effects of epidermal growth factor on the composition, structure, and function of the subventricular zone and rostral migratory stream in the normal and irradiated brain. Epidermal growth factor signaling is present in numerous cell types and regulates processes during development, tissue homeostasis, and disease. We sought out to study the following aspects of epidermal growth factor-treatment of the rodent brain:

- Structural changes in the subventricular zone as a result of EGF-treatment

- Cellular composition and growth dynamics of EGF-induced subventricular zone polyps

- The functional and structural response of the rostral migratory stream to EGF-treatment

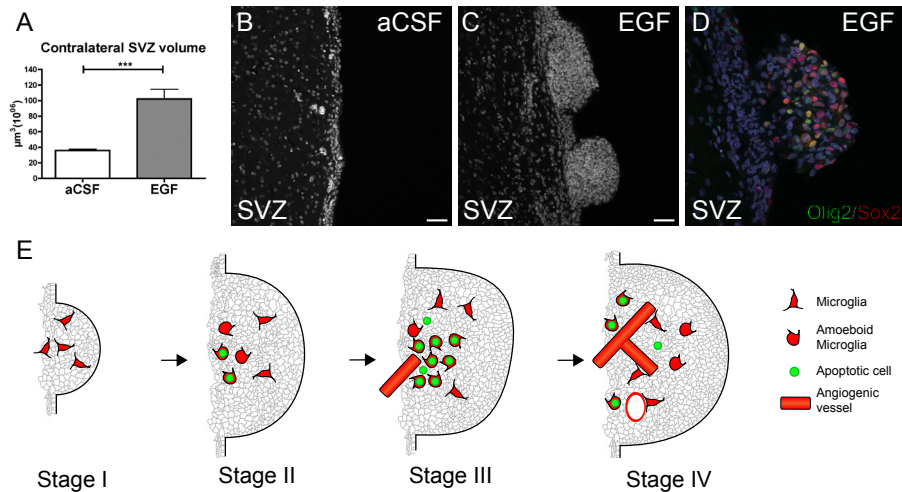- Acute and late effects of EGF in the subventricular zone after postnatal whole brain irradiation

RESULTS AND DISCUSSION

ICV infusion of EGF leads to structural changes in the SVZ and the RMS (Paper I and III)

In Paper I, we measured the volume of the SVZ following 14 days of EGF infusion. Since the cerebroventricular system is interconnected both the ipsi and contralateral SVZ are exposed to the infused agent; however, the concentration is presumably lower on the contralateral side. Nevertheless, to avoid confounding effects due to cannula placement, we measured the volume of the SVZ on the contralateral side. We found a three-fold increase in the size of the contralateral SVZ after 14 days of EGF infusion (Figure 4A). Apart from a general thickening of the EGF-treated SVZ compared to control (Figure 4B and C), polyp-like structures protruded from the SVZ (Figure 4C), as previously reported (Kuhn et al., 1997, Ninomiya et al., 2006, de Chevigny et al., 2008, Sun et al., 2010).

Extensive proliferation occurs in the RMS, the migratory pathway to the olfactory bulb and the RMS appears to contain stem cells, much like the SVZ (Gritti et al., 2002, Coskun et al., 2007, Alonso et al., 2008, Giachino and Taylor, 2009). It has been previously described how EGF infusion leads to decreased olfactory bulb neurogenesis and reduced proliferation in the RMS (Kuhn et al., 1997). However, more detailed analysis of the effects of EGF infusion on the RMS is lacking. In Paper III, we studied the density and cross-sectional area of the proximal and distal RMS (in relation to the cerebral ventricles) following EGF infusion. The proximal RMS was less dense and had a bigger cross-sectional area in the EGF-infused animals. Only minor effects were observed in the distal RMS where the density was reduced. These results indicate an expansion of the SVZ and dispersion of the proximal RMS. Apart from a cellular expansion, previous reports have demonstrated significant infiltration of SVZ cells into the parenchyma following EGF-infusion (Kuhn et al., 1997, Doetsch et al., 2002). In mice, EGF-infusion induces upregulation of the ECM molecule tenascin-C, indicating dynamic changes in the ECM that promote cellular motility (Doetsch et al., 2002). Such increased expression of ECM molecules in the SVZ and RMS could cause the atypical infiltration of cells into the sur-

rounding parenchyma observed after EGF infusion. Furthermore, similar to our results, inactivation of the EGFR family member ErbB4 induced altered migratory behavior with retention of stem and progenitor cells in the SVZ, and accumulation and dispersion of cells in the RMS (Ghashghaei et al., 2006).

Figure 4.

Effects of epidermal growth factor (EGF) in the subventricular zone (SVZ) and rostral migratory stream (RMS). (A) Total volume of the contralateral SVZ. (B) Vehicle-treated (aCSF) SVZ. (C) Enlarged SVZ and polyps of EGF-treated SVZ following 14 days of infusion. (D) Olig2 (green) and Sox2 (red) expression in polyps demonstrating coexpression in dysplastic cells. (E) Graphical illustration of polyp progression. Scale bars for B and C 50µm

EGF induces the formation of SVZ dysplastic polyps (Paper I)

In Paper I we characterized ultrastructure and protein expression of cells found within the EGF-induced polyps. After 14 days of EGF infusion polyps ranging in size from ~25µm to ~1mm in diameter are observed. Using scanning electron microscopy (SEM) we could demonstrate absence of an ependymal cell layer on the surface of the polyps. In contrast to the lateral ventricle wall of vehicle-treated animals covered with ciliated ependymal cells, the outermost cell layer of the polyps was composed of unciliated cells rich in excess membrane. Using transmission electron microscopy (TEM) analysis we discerned distinct ultrastructural properties of the cells within the polyps. Salient features of polyp cells were light nuclei with predominant euchromatin, an abundance of ribosomes, invaginated nuclei and reticulated nucleoli. Cells with similar

EM-characteristics were described by Peretto and colleagues in the postnatal RMS (Peretto et al., 2005). Light cells with large, occasionally invaginated nuclei were identified as cells of immature glial phenotype.

To further characterize the lineage and maturity of the polyp cells we used a broad panel of markers for stem and progenitor cells, glial cells, neuronal precursors, and OPCs. Expression of nestin, GFAP, vimentin, and Sox2, markers of astrocytes and radial glia, was detected in close to half of the cells, significantly more frequent compared to the control SVZ. Of these markers, Sox2 was the most frequently expressed, found in over 60% of polyp cells. During development, Sox2 is thought to prevent differentiation of neural progenitor cells to motor neurons in the spinal cord. Forced expression of Sox2 maintains the neural progenitor cells in an immature state (Graham et al., 2003). EGFR-mediated signaling can promote Sox2 expression, and Sox2 in turn can upregulate EGFR-expression by binding to the EGFR promoter. Inhibition of PI3K and MAPK signaling completely abolish the dedifferentiating effects of Sox2 (Hu et al., 2010). Expression of Olig2 was increased ten-fold in the polyps, much like previous studies performed in the SVZ of mice (Gonzalez-Perez et al., 2009). Inhibiting Olig2 expression in embryonic neurospheres greatly reduces the numbers of neurospheres generated. Moreover, addition of EGF in neurosphere cultures increases the number of Olig2-expressing cells (Hack et al., 2005). Following injury, reactive astrocytes acquire Olig2 expression, but not expression of OPC markers NG2 and PDGFRα (Buffo et al., 2005). Conditional deletion of Olig2 reduces the numbers of reactive astrocytes and proliferating cells after cortical injury (Chen et al., 2008). Unlike the EGF-treated mouse SVZ, we found only scarce expression of NG2, both in polyps and control SVZ. This suggests a more immature OPC-like phenotype of EGF-stimulated cells in the rat SVZ. Alternatively, the cells have more in common with reactive astrocytes. Interestingly, inhibition of Olig2 in reactive astrocytes increases the neurogenic potential of these cells (Buffo et al., 2005).

Analyzing coexpression of DCX, GFAP, nestin, NG2, Olig2, and Sox2, we found a subset of cells expressing Sox2$^+$/Olig2$^+$. Coexpression of Sox2 and Olig2 was highly enriched in the polyps (Figure 4D), but rarely found in the control SVZ. The ultrastructural characteristics and protein expression pattern

of cells found in the polyps indicate the presence of a EGF-expanded dysplastic cell type not found in the normal SVZ, resembling immature glial cells of the developing brain. Our previous analyses suggest that the dysplastic cell type is immature, metabolically active, and glial-like, but the proliferative potential of the cell was unknown. We therefore analyzed the proportion of Sox2 and Olig2 expression in proliferating cells. Within the population of cells expressing the M-phase marker phospho-histone H3 (pHH3), Sox2 was enriched two-fold after EGF treatment. Furthermore, Olig2 expression was three times as frequent in proliferating cells in EGF-stimulated SVZ compared to control. Judging from the proliferative nature of Sox2 and Olig2 expressing cells we can assume that the dysplastic cells induced by EGF-infusion are the main contributors to the formation and expansion of the SVZ polyps.

Gradual microglia accumulation and angiogenesis indicate discrete stages of polyp development (Paper II)

Comparing polyps following 7 and 14 days of EGF infusion demonstrated a three-fold increase in size after 14 days compared to 7 days of infusion. Moreover, polyps formed after 14 days of EGF infusion occasionally displayed extensive vascularization in the polyp core. No vascularized polyps were found after 7 days of EGF infusion. Infusion of EGFR ligand TGF-α has been linked to microglia accumulation in the SVZ (de Chevigny et al., 2008). Studying microglia in polyps, using an antibody against Iba1 revealed different degrees of accumulation and activation in polyps following 7 and 14 days of EGF infusion. Comparing microglial response and vascularization in polyps formed after 7 and 14 days of EGF infusion, four distinct stages of polyps became apparent. Stage I polyps were often small protrusions from the SVZ and putatively the most recently formed polyps, with microglial density and appearance similar to the control SVZ. Stage II polyps had a spherical shape and exhibited microglia accumulation in the core. Stage III polyps had extensive microglial accumulation, an abundance of microglia with a round phagocytic morphology, and occasionally single vessels leading into the polyp core. Stage IV polyps were characterized by a prominent vascular plexus in the polyp core and often covering extensive stretches of SVZ.

Using the defined criteria to compare polyp size between the stages we found a continuous increase from stage I-IV. Furthermore, a noticeable three-fold increase in polyp size was observed from stage III to stage IV, a transition defined by polyp vascularization, suggesting angiogenesis to be essential for cell expansion beyond a certain size. The morphology of individual microglia was greatly altered from an amoeboid phagocytic appearance, in stage III polyps, to a ramified morphology in the vascularized stage IV polyps. Moreover, microglia in vascularized stage IV polyps were found closely associated with newly formed vessels. Differences in microglia morphology in polyps of different stages suggested an involvement of microglia in polyp progression. In the retina, microglia are tightly associated with developing vessels and loss of microglia leads to reduced angiogenesis during development (Checchin et al., 2006). Measuring microglia density in polyps we found an increase from stage I-III, however comparing stage III to stage IV there was a considerable reduction in microglia density. This dynamic behavior could be explained by increasing polyp tissue reactivity and inflammation, followed by microglia invasion. Subsequent secretion of proteases and pro-angiogenic factors by microglia could stimulate endothelial cell proliferation and migration, followed by microglia deactivation (summarized in Figure 4E). A similar model has been proposed for macrophage-induced angiogenesis through regulation of Wnt5 (Newman and Hughes, 2012).

The rapid growth of the polyps and the accumulation of microglia could be associated with increased apoptosis. When we assessed cell death, the density of ApopTAG-positive cells in the polyps followed a pattern similar to the accumulation of microglia. Apoptotic cells were rarely found in stage I and stage II polyps. The density of apoptotic cells increased almost 20-fold from stage II to stage III. At stage IV the apoptosis had declined sharply to one third of the level found at stage III. The close association of apoptosis and microglia accumulation in the polyps indicates a synergistic involvement of the two cell populations in the induction of angiogenesis. Apoptotic cells have been described to be capable of reprogramming macrophages to angiogenesis-promoting cells that secrete pro-angiogenic factors (Weis et al., 2009, Brecht et al., 2011). The substantial polyp growth and reduction of microglia associated with angiogenesis during the transition from stage III to IV indicates a dependency on vascu-

larization for extensive growth and a role of microglia in the angiogenic process initiated at stage III. A possible scenario is that hypoxia is locally induced in the expanded, but avascular polyps in stage III, followed by apoptosis, which prevents further growth and causes microglia accumulation. Upon angiogenesis the local oxygen tension is increased, resulting in microglia normalization, followed by further growth and decline of apoptosis from stage III to stage IV.

Altered cell composition in the EGF treated RMS (Paper III)

In coronal sections of the vehicle-treated control RMS, DCX-expressing neuroblasts were organized in chains with a few cells in diameter and hundreds of chains making up the entire RMS. In the EGF-treated RMS there were fewer neuroblasts and the morphology was less organized and overall a reduced number of chains were detected. In the EGF-treated SVZ, atypical clusters of neuroblasts were frequently observed. Instead of an even distribution along the dorso-ventral axis of the SVZ, neuroblasts in the EGF-treated SVZ were predominately found in clusters (Figure 5A). These clusters bear resemblance to the masses of neuroblast present in the early postnatal RMS (Peretto et al., 2005). In the postnatal RMS, neuroblasts migrate in large masses rather than in discrete chains. Whether the neuroblasts in the EGF-treated SVZ cluster as a result of adopting a more immature phenotype or because of inhibitory signals as a result of EGF infusion remains to be investigated. In the normal RMS a subset of neuroblasts express EGFR and migrate slower and in a more irregular fashion. EGFR stimulation using TGF-α reduced the motility of EGFR expressing neuroblasts (Kim et al., 2009). One explanation for the EGF-induced neuroblast clustering could be selective stimulation of the EGFR-positive neuroblast population resulting in halted migration of this neuroblast subset.

Our group has previously characterized the expression of the ERM (ezrin-radixin-moesin) family of proteins in the adult brain (Persson et al., 2010). Two cell types express the cytoskeleton anchor protein radixin in the adult brain, neuroblasts of the hippocampus, SVZ, and RMS as well as Olig2-positive OPCs that are found throughout the brain. We quantified DCX and Olig2 expression in radixin+ cells of the EGF-treated RMS. After 7 days of EGF infusion the percentage of radixin cells expressing DCX in the RMS was reduced to half of

the control (Figure 5B and C). The reduction in radixin+/DCX+ cells was even more prominent after 14 days of EGF infusion, when the percentage of cells coexpressing radixin and DCX (radixin+/DCX+) drops to less than one tenth of the control RMS. Interestingly, a reciprocal increase in the population of radixin+/Olig2+ cells was observed in the EGF-stimulated RMS. Coexpression of radixin and Olig2 was only found in a few percent of cells in the control RMS (Figure 5E), cells presumably phenotypically similar to the radixin+/Olig2+ OPCs found throughout the normal brain. In contrast, the percentage of radixin+/Olig2+ cells increased ten-fold during 7 days of EGF infusion (Figure 5F). Unlike the decline in radixin+/DCX+ cells, no further increase in radixin+/Olig2+ cells was found after 14 days of EGF treatment. Studying the expression of GFAP, CNPase, NG2, and Iba1 in the EGF-treated RMS, no differences were found in the resident astrocyte, OPC, or microglia populations. Interestingly, the Sox2 expression pattern in the EGF-treated RMS appeared upregulated, again similar to what we describe in polyps in Paper I. Moreover, three quarters of radixin+/Olig2+ cells in the EGF stimulated RMS expressed Sox2. This suggests that expansion of the EGF-induced dysplastic cell in the SVZ is also present in the RMS. Moreover, studying radixin expression in the control and EGF-treated SVZ revealed extensive expression in EGF-induced polyps (Figure 5D and G).

Members of the ERM family are expressed in the developing brain of both humans and rodents (Johnson et al., 2002, Gimeno et al., 2004). In rats, expression of ERM peaks in the late embryonic early postnatal brain (Paglini et al., 1998), and ERMs are also implicated in tumor development (Kinoshita et al., 2012, Wang et al., 2012, Zhu et al., 2013). Together these results suggest than ERMs are important in developmental processes, where active cytoskeleton restructuring is important. We recently demonstrated how chemical inhibition of radixin reduced neuroblast migration *in vitro* in a dose dependent manner, while glial migration was not affected. *In vivo* inhibition of radixin led to aberrant neuroblast chain assembly, RMS migration, and proliferation (Persson et al., 2013). The effects of EGF on upregulation of radixin in Olig2+ cells are most likely indirect, a result of the dysplastic changes induced by EGF.

The expanded population of radixin+/Olig2+ cells could originate from cells in the RMS or migrate from the SVZ or other parts of the brain aggregating in

the RMS. To test this we infused EGF for 24 hours, during which three injections of BrdU were administered. Quantifying BrdU and Olig2 coexpression at two different rostro-caudal locations in the RMS after 24 hours of EGF infusion revealed an increase in the percentage of Olig2 expressing cells within the proliferating population in both the distal and proximal RMS. This suggests that the expanded Olig2 population originates locally in the RMS.
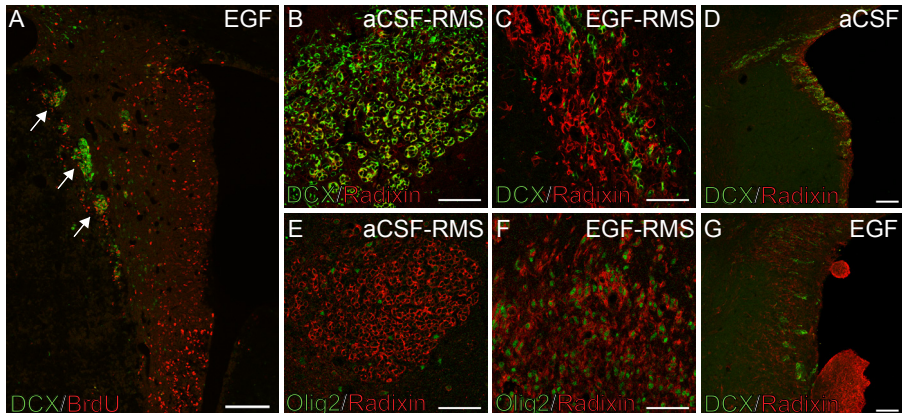
Figure 5.
Neuroblast clusters (arrows) in EGF-treated subventricular zone (SVZ) labeled by DCX (green) and proliferating cells labeled using BrdU in (red). (B and C) representative images of DCX (green) and radixin (red) in control (B) and EGF-treated (C) rostral migratory stream (RMS). (D) Expression of DCX and radixin in the control SVZ. (E and F) Representative images of Olig2 (green) and radixin (red) in control (E) and EGF-treated (F) RMS. (G) Expression of DCX and radixin in the EGF-treated subventricular zone (SVZ) showing scattered DCX-expressing neuroblasts and extensive radixin immunoreactivity in polyps. Scale bar in A 100μm, B-G 50μm

Although different in cell composition and structure the SVZ and the RMS react similarly to EGF stimulation. In the early postnatal brain a subset of NG2-expressing OPCs in the SVZ and RMS express the EGFR and migrate under EGF stimulation *in vitro*. Overexpression of human EGFR under control of the oligodendrocyte lineage promoter Cnp in cortical NG2 cells confers migratory properties to otherwise non-migratory OPCs. Moreover, EGF-stimulated migration only occurs in the presence of ECM molecules (Aguirre et al., 2005). Moreover, migration of NG2 expressing cells has been induced in adult mice, although following chemical demyelination (Aguirre et al., 2007). Based on our results we can hypothesize that, in the absence of an

injury, the SVZ and RMS are the only structures in the adult brain providing the proper conditions to support EGF-induced glial migration.

Functional effects of EGF on migration *in vivo* and *in vitro* (Paper III)

Radixin is expressed by both neuroblasts and OPCs in the adult brain, cell types not only functionally different, but also of different lineages. Using an antibody against phosphorylated ERM (pERM) together with antibodies against radixin, we studied radixin activation in the two radixin-expressing cell populations. In the control RMS, pERM was frequently expressed by radixin$^+$/DCX$^+$ neuroblasts, however rarely in the radixin$^+$/Olig2$^+$ OPCs. Analysis of the EGF-expanded population of radixin$^+$/Olig2$^+$cells revealed extensive pERM expression. Interestingly, radixin$^+$/Olig2$^+$ cells occasionally organized in chain-like structures along the rostro-causal axis of the RMS and expressed pERM. The morphology and the presence of phosphorylated (activated) radixin in the EGF-expanded radixin$^+$/Olig2$^+$ cells suggest migratory properties.

To further study the migratory potential of radixin$^+$/Olig2$^+$ cells, we employed *in vitro* SVZ explant cultures. Small pieces of the SVZ were placed in artificial ECM and the cells migrating away from the explants were analyzed. The majority of cells migrating out from the explants expressed radixin, and a subset of these cells coexpressed Olig2. In addition, the migratory radixin$^+$/Olig2$^+$ cells displayed radixin activation in the form of pERM expression, possibly implying migratory capabilities of EGF-expanded radixin$^+$/Olig2$^+$ cells *in vivo*. Phosphorylation of ERM proteins leads to a conformational change that allows binding to the actin cytoskeleton and actin polymerization (Fehon et al., 2010). The same mechanism could potentially be induced *in vivo* by EGF-stimulation in Olig2$^+$ cells conferring migratory potential to otherwise stationary cells.

SVZ gene expression analysis confirms neuroblast reduction and reveals differential regulation of Inhibitor of DNA-binding genes (Paper I and III)

In Paper I and III we quantified mRNA expression in the SVZ and olfactory bulb after 14 days of EGF infusion. Whole SVZ and olfactory bulb were micro-

dissected from the ipsi- and contralateral side and mRNA expression was measured using real-time RT-PCR. *Egfr* mRNA expression was increased more than six-fold in the EGF-treated SVZ. EGFR is predominantly expressed by SVZ C-cells, but has also been found in astrocytes, ependymal cells, and a subset of neuroblasts (Doetsch et al., 2002, Danilov et al., 2009, Kim et al., 2009).

The reduction in neuroblasts observed on a cellular level in the SVZ (Paper I) and RMS (Paper III) was corroborated by a reduction in *Dcx* expression in the SVZ and the olfactory bulb. Radixin expression was increased in the SVZ and unchanged in the olfactory bulb following EGF infusion, confirming that, although *radixin* and *Dcx* are mainly expressed by neuroblasts in the naïve brain, the expression of the two genes responds differently to EGF treatment. The reduction in neuroblasts in the SVZ and RMS described above, could lead to an increased homogeneity of the EGF-stimulated SVZ, composed predominately of EGF-responsive cells, resulting in a general increase in the *Egfr* mRNA expression.

bHLH transcription factors are critical regulators of neural development in the developing and adult brain (Yun et al., 2002, Roybon et al., 2009). Inhibitor of DNA binding (Id) proteins alter the activity of bHLH transcription factors by binding competitively to E-proteins, preventing the E-proteins to act as transcriptional activators (Ruzinova and Benezra, 2003). *Id*-genes are specifically expressed in neural stem cells and are critical for regulating critical stem cell functions such as self-renewal capacity (Nam and Benezra, 2009). We quantified the relative mRNA expression of *Id1*, *2*, and *4* in the EGF-treated SVZ. *Id1*, expressed by B-cells and C-cells in the SVZ (Nam and Benezra, 2009), was upregulated two-fold following EGF infusion. In contrast, expression of *Id2* and *Id4* was downregulated as a result of EGF treatment. Overexpression of both *Id2* and *Id4* leads to inhibition of oligodendrocyte differentiation (Kondo and Raff, 2000, Wang et al., 2001). The differential regulation of *Id*-genes in the EGF-stimulated SVZ suggests an increase in genes promoting stemness (*Id1*) and a reduction in the expression of genes maintaining OPC immaturity (*Id2* and *Id4*). This fits nicely with the previously established ultrastructural and phenotypic characterization of the cells in the EGF-stimulated SVZ, being immature glial cells not displaying OPC markers other than Olig2 expression.

Stimulatory, age-dependent effects of EGF on the irradiated SVZ (Paper IV)

In order to compare EGF effects in the juvenile and adult brain after irradiation, we performed in Paper IV irradiation at P9 followed by EGF infusion at P21 or P80. When analyzing naïve sham-irradiated animals, EGF treatment in juvenile animals increased the SVZ volume compared to vehicle controls, while the density of proliferating cells was unchanged. In contrast to the adult brain, not even the frequency of cells expressing Sox2, Olig2, or DCX was altered after EGF treatment. Prior irradiation expectedly resulted in a reduction of SVZ size in vehicle infused juvenile animals. EGF-treatment of the irradiated SVZ expanded the size to the level of the control SVZ. The density of proliferating cells was negatively affected by irradiation which was reduced in both vehicle and EGF-infused irradiated juvenile animals. Although the size of the SVZ was reduced in irradiated animals the ratio of cells expressing Sox2, Olig2, and DCX was the same in vehicle-treated irradiated and naïve animals, indicating that negative effects of irradiation does not appear to target a specific cell population. Surprisingly, the combination of irradiation and juvenile EGF infusion significantly reduced the ratio of cells expressing DCX. The ratio of DCX expressing cells was lower in irradiated EGF-infused animals compared to all other groups, while Olig2 and Sox2/Olig2 expression was increased. As no direct proliferative differences are found between EGF and vehicle-infused irradiated brains, one possible explanation for the discrepancy in SVZ volume could be increased survival. In this context it is interesting to note, that acute EGF treatment increases hematopoietic regeneration after whole-body irradiation through repression of the proapoptotic protein PUMA (Doan et al., 2013).

EGF infusion into the adult brain (P80) increased the volume of the naïve SVZ, similar to what we demonstrate in Paper I. Proliferation was not significantly different between vehicle and EGF-induced groups, although a trend towards increased density of proliferating cells was evident following EGF infusion. Moreover, the ratio of Sox2, Olig2, and Sox2/Olig2 expressing cells was elevated in EGF-infused animals, while DCX expression was reduced, again, similar to what we describe in Paper I. Adult animals that received postnatal irradiation did not display a reduction in SVZ volume after vehicle infusion at P80 and the density of proliferating cells was not markedly different between

the naïve and the irradiated animals. This indicates that the SVZ is largely recovered in terms of volume and proliferation around ten weeks after irradiation at P9. Previous studies from our group demonstrated that nine weeks after 6 Gy of irradiation proliferation in SVZ was half of the controls, after an initial drop to 10% of controls (Hellstrom et al., 2009). Comparing the mean values of the density of proliferating cells in our study between the two vehicle-treated groups the value of the irradiated SVZ is 64% of the proliferation compared to the naïve SVZ; although the data are not significant, this indicates a trend similar to the previously published data (Hellstrom et al., 2009).

Although EGF-infusion into the irradiated adult SVZ at P80 triggers a proliferative response in terms of SVZ expansion, the density of proliferating cells was not increased compared to vehicle-infused animals. The tissue-expanding effects of EGF on the irradiated SVZ in adult animals are thus not as prominent as after P21 infusion. Moreover, the cellular composition of the EGF-treated naïve SVZ at P21 and P80 are substantially different and the P21 EGF-treated SVZ is in several aspects very similar to the control SVZ. Distinct responses to EGFR overexpression are found in postnatal animals indicating a different role of EGF-signaling in the postnatal SVZ and RMS compared to the adult (Aguirre et al., 2005). Irradiation and aging have been suggested to result in similar detrimental effects on the adult SVZ (Pineda et al., 2013), it is therefore conceivable that irradiation prior to P21 infusion of EGF results in a more adult-like response to EGF.

Age and irradiation-related changes in polyp composition and proliferation (Paper IV)

In Paper I we describe how the EGF-induced dysplasia is particularly prominent in polyps. Therefore, we chose in this paper to analyze polyp proliferation and composition separately from the SVZ. EGF-induced polyps from the juvenile naïve SVZ were in several aspects distinct from their adult counterparts. Like the P21 SVZ, the P21 polyps were more proliferatively active compared to P80 polyps; however, the expression of both Sox2 and Olig2 was lower. Surprisingly, considerable DCX expression was found in P21 polyps, which we did not observe in adult animals. Interestingly, a combination of irradiation and

EGF infusion reduced the density of DCX expressing cells in the P21 polyps substantially. Although irradiation treatment reduced the proliferation in the P21 polyps, the ratios of Sox2 or Olig2 expressing cells were not altered in irradiated animals. Buthionine sulfoximine can reduce the levels of glutathione and creates an oxidative environment *in vitro* and *in vivo*. Treatment using buthionine sulfoximine in early postnatal animals reduced neurogenesis in favor for glial differentiation through the histone deacetylase Sirt1 (Prozorovski et al., 2008). Similar regulation could be involved in reducing neuroblasts in the P21 EGF-treated irradiated SVZ and polyps, which could be expected to be more oxidated due to ROS induced by irradiation. EGF infusion at P80 did not result in differences in proliferation or cellular composition compared to polyps in the irradiated to the sham-irradiated animals. Substantial Sox2 and Olig2 expression was found in polyps from both the naïve and irradiated SVZ, and DCX expressing cells were infrequent. Although similar in proliferation and composition, polyps from the irradiated P80 SVZ appear less frequently compared to EGF-treated naïve animals. This indicates that polyps are formed from highly proliferative EGF-responsive stem cells in the adult SVZ and once polyp formation is initiated, growth and cell composition of the polyps are similar to those of naive animals.

CONCLUSIONS

The contributions of the current thesis are two-fold. The results provide insight into the mechanisms regulating neural stem cell plasticity in the adult brain, but also highlights similarities between SVZ neurogenesis and brain tumor development.

Growth and survival factors are extensively studied for their therapeutic potential in neurological diseases. Treating neurodegenerative diseases and brain injury using neurotrophic factors like vascular endothelial growth factor (VEGF), BDNF, and erythropoietin (EPO) could reduce loss of cells and potentially ameliorate the disease progression (Bogaert et al., 2006, Jerndal et al., 2010, Nagahara and Tuszynski, 2011). Rather than expanding cell populations, these treatments aim at increasing cell survival in neurodegenerative diseases. From a therapeutic perspective, the proliferative effects of EGF could instead serve as a means to expand the neural stem and progenitor cell population. Newly generated cells could then potentially replace cells rather than prevent diseased cells from dying. In the current thesis, different aspects of the stimulatory effects of EGF are studied. We demonstrate how neural stem cell respond to EGF-infusion and expand in different regions of the brain even following irradiation. Furthermore, extensive expansion of cells in the SVZ can, at least temporarily, be sustained through angiogenesis. Continued efforts made into studying the microenvironment inside EGF-induced polyps could possibly help unlock the proliferative potential of the SVZ and RMS for regenerative purposes. Moreover, the ability of the RMS to respond locally to EGF-stimulation and expand a subset of migratory glial cells, suggests that cells can be generated throughout the RMS. Although, EGF-stimulation temporarily downregulates olfactory bulb neurogenesis and neuroblast development, a study demonstrated that, after EGFR stimulation ended, the newly generated cells can re-adopt a neuroblast fate (de Chevigny et al., 2008).

Neural stem cells share several properties with cells derived from glial tumors, such as glioma and ependymoma (Sanai et al., 2005, Taylor et al., 2005, Vescovi

et al., 2006). Both cell types express markers of immature glial cells, proliferate, can be cultured as spheres *in vitro*, and are regulated by similar mechanisms (Galli et al., 2004, Sanai et al., 2005, Ligon et al., 2007). We describe how EGF-infusion leads to formation of tumor-like polyps enriched in dysplastic cells. During prolonged treatment, polyps are invaded by microglial cells and acquire angiogenesis. However, upon growth factor withdrawal the polyps regress and the SVZ appear to normalize (Kuhn et al., 1997), possibly due to active elimination of cells via cell death as shown in Paper II. Apoptosis-deficient neural stem cells transfected with constituently active EGFR can generate glial tumors *in vivo* (Bachoo et al., 2002), indicating that both mitotic signaling as well as cell death mechanisms need to be altered for continuous aberrant growth. The here-developed model of subependymal polyp generation by EGF could represent a reversible premalignant stage of tumor development. Moreover, our results suggest that properties formerly attributed to tumor cells, such as angiogenesis, can be induced in the neurogenic niche. This indicates that some differences between stem cells and tumor cells could be context-dependent rather than cell-intrinsic. Furthermore, our results demonstrate the importance of non-neurogenic cell types in the SVZ niche in the progression of the polyps. Genetic manipulation of neural stem cells, microglia, or endothelial cells in the SVZ combined with EGF infusion could result in non-reversible neoplasms. The EGF-infusion model could thus be useful for our understanding of the events that precede the cancer-initiating event.

REFERENCES

Achanta, P., Capilla-Gonzalez, V., Purger, D., Reyes, J., Sailor, K., Song, H., Garcia-Verdugo, J.M., Gonzalez-Perez, O., Ford, E., and Quinones-Hinojosa, A. (2012). Subventricular zone localized irradiation affects the generation of proliferating neural precursor cells and the migration of neuroblasts. Stem Cells 30, 2548-2560.

Adachi, K., Mirzadeh, Z., Sakaguchi, M., Yamashita, T., Nikolcheva, T., Gotoh, Y., Peltz, G., Gong, L., Kawase, T., Alvarez-Buylla, A., Okano, H., and Sawamoto, K. (2007). Beta-catenin signaling promotes proliferation of progenitor cells in the adult mouse subventricular zone. Stem Cells 25, 2827-2836.

Aguirre, A., Dupree, J.L., Mangin, J.M., and Gallo, V. (2007). A functional role for EGFR signaling in myelination and remyelination. Nat Neurosci 10, 990-1002.

Aguirre, A., Rizvi, T.A., Ratner, N., and Gallo, V. (2005). Overexpression of the epidermal growth factor receptor confers migratory properties to nonmigratory postnatal neural progenitors. J Neurosci 25, 11092-11106.

Aguirre, A., Rubio, M.E., and Gallo, V. (2010). Notch and EGFR pathway interaction regulates neural stem cell number and self-renewal. Nature 467, 323-327.

Alonso, M., Ortega-Perez, I., Grubb, M.S., Bourgeois, J.P., Charneau, P., and Lledo, P.M. (2008). Turning astrocytes from the rostral migratory stream into neurons: a role for the olfactory sensory organ. J Neurosci 28, 11089-11102.

Altman, J. (1969). Autoradiographic and histological studies of postnatal neurogenesis. IV. Cell proliferation and migration in the anterior forebrain, with special reference to persisting neurogenesis in the olfactory bulb. J Comp Neurol 137, 433-457.

Andres-Barquin, P.J., Hernandez, M.C., and Israel, M.A. (1998). Injury selectively down-regulates the gene encoding for the Id4 transcription factor in primary cultures of forebrain astrocytes. Neuroreport 9, 4075-4080.

Azzam, E.I., Jay-Gerin, J.P., and Pain, D. (2012). Ionizing radiation-induced metabolic oxidative stress and prolonged cell injury. Cancer Lett 327, 48-60.

Bachoo, R.M., Maher, E.A., Ligon, K.L., Sharpless, N.E., Chan, S.S., You, M.J.,

Tang, Y., Defrances, J., Stover, E., Weissleder, R., Rowitch, D.H., Louis, D.N., and Depinho, R.A. (2002). Epidermal growth factor receptor and Ink4a/Arf: convergent mechanisms governing terminal differentiation and transformation along the neural stem cell to astrocyte axis. Cancer Cell 1, 269-277.

Balbis, A., Parmar, A., Wang, Y., Baquiran, G., and Posner, B.I. (2007). Compartmentalization of signaling-competent epidermal growth factor receptors in endosomes. Endocrinology 148, 2944-2954.

Basak, O., Giachino, C., Fiorini, E., Macdonald, H.R., and Taylor, V. (2012). Neurogenic subventricular zone stem/progenitor cells are Notch1-dependent in their active but not quiescent state. J Neurosci 32, 5654-5666.

Bastien-Dionne, P.O., David, L.S., Parent, A., and Saghatelyan, A. (2010). Role of sensory activity on chemospecific populations of interneurons in the adult olfactory bulb. J Comp Neurol 518, 1847-1861.

Batzer, A.G., Rotin, D., Urena, J.M., Skolnik, E.Y., and Schlessinger, J. (1994). Hierarchy of binding sites for Grb2 and Shc on the epidermal growth factor receptor. Mol Cell Biol 14, 5192-5201.

Bergmann, O., Liebl, J., Bernard, S., Alkass, K., Yeung, M.S., Steier, P., Kutschera, W., Johnson, L., Landen, M., Druid, H., Spalding, K.L., and Frisen, J. (2012). The age of olfactory bulb neurons in humans. Neuron 74, 634-639.

Bergonie, J., and Tribondeau, L. (1959). Interpretation of some results of radiotherapy and an attempt at determining a logical technique of treatment. Radiat Res 11, 587-588.

Berridge, M.J., Lipp, P., and Bootman, M.D. (2000). The versatility and universality of calcium signalling. Nat Rev Mol Cell Biol 1, 11-21.

Bieberich, E. (2012). It's a lipid's world: bioactive lipid metabolism and signaling in neural stem cell differentiation. Neurochem Res 37, 1208-1229.

Bingle, L., Brown, N.J., and Lewis, C.E. (2002). The role of tumour-associated macrophages in tumour progression: implications for new anticancer therapies. J Pathol 196, 254-265.

Bogaert, E., Van Damme, P., Van Den Bosch, L., and Robberecht, W. (2006). Vascular endothelial growth factor in amyotrophic lateral sclerosis and other neurodegenerative diseases. Muscle Nerve 34, 391-405.

Bonfanti, L. (2006). PSA-NCAM in mammalian structural plasticity and neurogenesis. Prog Neurobiol 80, 129-164.

Brecht, K., Weigert, A., Hu, J., Popp, R., Fisslthaler, B., Korff, T., Fleming, I.,

Geisslinger, G., and Brune, B. (2011). Macrophages programmed by apoptotic cells promote angiogenesis via prostaglandin E2. FASEB J 25, 2408-2417.

Brown, J.P., Couillard-Despres, S., Cooper-Kuhn, C.M., Winkler, J., Aigner, L., and Kuhn, H.G. (2003). Transient expression of doublecortin during adult neurogenesis. J Comp Neurol 467, 1-10.

Buck, L.B. (2004). The search for odorant receptors. Cell 116, S117-119, 111 p following S119.

Buffo, A., Vosko, M.R., Erturk, D., Hamann, G.F., Jucker, M., Rowitch, D., and Gotz, M. (2005). Expression pattern of the transcription factor Olig2 in response to brain injuries: implications for neuronal repair. Proc Natl Acad Sci U S A 102, 18183-18188.

Cadigan, K.M., and Nusse, R. (1997). Wnt signaling: a common theme in animal development. Genes Dev 11, 3286-3305.

Carleton, A., Petreanu, L.T., Lansford, R., Alvarez-Buylla, A., and Lledo, P.M. (2003). Becoming a new neuron in the adult olfactory bulb. Nat Neurosci 6, 507-518.

Chattopadhyay, A., Vecchi, M., Ji, Q., Mernaugh, R., and Carpenter, G. (1999). The role of individual SH2 domains in mediating association of phospholipase C-gamma1 with the activated EGF receptor. J Biol Chem 274, 26091-26097.

Checchin, D., Sennlaub, F., Levavasseur, E., Leduc, M., and Chemtob, S. (2006). Potential role of microglia in retinal blood vessel formation. Invest Ophthalmol Vis Sci 47, 3595-3602.

Chen, Y., Miles, D.K., Hoang, T., Shi, J., Hurlock, E., Kernie, S.G., and Lu, Q.R. (2008). The basic helix-loop-helix transcription factor olig2 is critical for reactive astrocyte proliferation after cortical injury. J Neurosci 28, 10983-10989.

Cohen, S. (1959). Purification and metabolic effects of a nerve growth-promoting protein from snake venom. J Biol Chem 234, 1129-1137.

Cohen, S. (1962). Isolation of a mouse submaxillary gland protein accelerating incisor eruption and eyelid opening in the new-born animal. J Biol Chem 237, 1555-1562.

Cohen, S. (1965). The stimulation of epidermal proliferation by a specific protein (EGF). Dev Biol 12, 394-407.

Cohen, S., and Levi-Montalcini, R. (1957). Purification and properties of a nerve

growth-promoting factor isolated from mouse sarcoma 180. Cancer Res 17, 15-20.

Cook, P.W., Piepkorn, M., Clegg, C.H., Plowman, G.D., Demay, J.M., Brown, J.R., and Pittelkow, M.R. (1997). Transgenic expression of the human amphiregulin gene induces a psoriasis-like phenotype. J Clin Invest 100, 2286-2294.

Cooper, J.A. (2013). Cell biology in neuroscience: Mechanisms of cell migration in the nervous system. J Cell Biol 202, 725-734.

Coskun, V., Falls, D.L., Lane, R., Czirok, A., and Luskin, M.B. (2007). Subventricular zone neuronal progenitors undergo multiple divisions and retract their processes prior to each cytokinesis. Eur J Neurosci 26, 593-604.

Craig, C.G., Tropepe, V., Morshead, C.M., Reynolds, B.A., Weiss, S., and Van Der Kooy, D. (1996). In vivo growth factor expansion of endogenous subependymal neural precursor cell populations in the adult mouse brain. J Neurosci 16, 2649-2658.

Cremer, H., Lange, R., Christoph, A., Plomann, M., Vopper, G., Roes, J., Brown, R., Baldwin, S., Kraemer, P., Scheff, S., and Et Al. (1994). Inactivation of the N-CAM gene in mice results in size reduction of the olfactory bulb and deficits in spatial learning. Nature 367, 455-459.

Curtis, M.A., Kam, M., Nannmark, U., Anderson, M.F., Axell, M.Z., Wikkelso, C., Holtas, S., Van Roon-Mom, W.M., Bjork-Eriksson, T., Nordborg, C., Frisen, J., Dragunow, M., Faull, R.L., and Eriksson, P.S. (2007). Human neuroblasts migrate to the olfactory bulb via a lateral ventricular extension. Science 315, 1243-1249.

Danilov, A.I., Gomes-Leal, W., Ahlenius, H., Kokaia, Z., Carlemalm, E., and Lindvall, O. (2009). Ultrastructural and antigenic properties of neural stem cells and their progeny in adult rat subventricular zone. Glia 57, 136-152.

De Chevigny, A., Cooper, O., Vinuela, A., Reske-Nielsen, C., Lagace, D.C., Eisch, A.J., and Isacson, O. (2008). Fate mapping and lineage analyses demonstrate the production of a large number of striatal neuroblasts after transforming growth factor alpha and noggin striatal infusions into the dopamine-depleted striatum. Stem Cells 26, 2349-2360.

Dhein, J., Walczak, H., Baumler, C., Debatin, K.M., and Krammer, P.H. (1995). Autocrine T-cell suicide mediated by APO-1/(Fas/CD95). Nature 373, 438-441.

Doan, P.L., Himburg, H.A., Helms, K., Russell, J.L., Fixsen, E., Quarmyne,

M., Harris, J.R., Deoliviera, D., Sullivan, J.M., Chao, N.J., Kirsch, D.G., and Chute, J.P. (2013). Epidermal growth factor regulates hematopoietic regeneration after radiation injury. Nat Med 19, 295-304.

Doetsch, F., Caille, I., Lim, D.A., Garcia-Verdugo, J.M., and Alvarez-Buylla, A. (1999a). Subventricular zone astrocytes are neural stem cells in the adult mammalian brain. Cell 97, 703-716.

Doetsch, F., Garcia-Verdugo, J.M., and Alvarez-Buylla, A. (1997). Cellular composition and three-dimensional organization of the subventricular germinal zone in the adult mammalian brain. J Neurosci 17, 5046-5061.

Doetsch, F., Garcia-Verdugo, J.M., and Alvarez-Buylla, A. (1999b). Regeneration of a germinal layer in the adult mammalian brain. Proc Natl Acad Sci U S A 96, 11619-11624.

Doetsch, F., Petreanu, L., Caille, I., Garcia-Verdugo, J.M., and Alvarez-Buylla, A. (2002). EGF converts transit-amplifying neurogenic precursors in the adult brain into multipotent stem cells. Neuron 36, 1021-1034.

Durocher, D., and Jackson, S.P. (2001). DNA-PK, ATM and ATR as sensors of DNA damage: variations on a theme? Curr Opin Cell Biol 13, 225-231.

Emsley, J.G., and Hagg, T. (2003). alpha6beta1 integrin directs migration of neuronal precursors in adult mouse forebrain. Exp Neurol 183, 273-285.

Eriksson, P.S., Perfilieva, E., Bjork-Eriksson, T., Alborn, A.M., Nordborg, C., Peterson, D.A., and Gage, F.H. (1998). Neurogenesis in the adult human hippocampus. Nat Med 4, 1313-1317.

Farah, M.H., Olson, J.M., Sucic, H.B., Hume, R.I., Tapscott, S.J., and Turner, D.L. (2000). Generation of neurons by transient expression of neural bHLH proteins in mammalian cells. Development 127, 693-702.

Fehon, R.G., Mcclatchey, A.I., and Bretscher, A. (2010). Organizing the cell cortex: the role of ERM proteins. Nat Rev Mol Cell Biol 11, 276-287.

Franco, S.J., and Muller, U. (2011). Extracellular matrix functions during neuronal migration and lamination in the mammalian central nervous system. Dev Neurobiol 71, 889-900.

Friedberg, E.C., Mcdaniel, L.D., and Schultz, R.A. (2004). The role of endogenous and exogenous DNA damage and mutagenesis. Curr Opin Genet Dev 14, 5-10.

Fukuda, A., Fukuda, H., Swanpalmer, J., Hertzman, S., Lannering, B., Marky, I., Bjork-Eriksson, T., and Blomgren, K. (2005). Age-dependent sensitivity of the developing brain to irradiation is correlated with the number and

vulnerability of progenitor cells. J Neurochem 92, 569-584.

Galli, R., Binda, E., Orfanelli, U., Cipelletti, B., Gritti, A., De Vitis, S., Fiocco, R., Foroni, C., Dimeco, F., and Vescovi, A. (2004). Isolation and characterization of tumorigenic, stem-like neural precursors from human glioblastoma. Cancer Res 64, 7011-7021.

Gavrieli, Y., Sherman, Y., and Ben-Sasson, S.A. (1992). Identification of programmed cell death in situ via specific labeling of nuclear DNA fragmentation. J Cell Biol 119, 493-501.

Gerbin, C.S. (2010). Activation of ERBB Receptors. Nature Education 3, 35.

Ghashghaei, H.T., Weber, J., Pevny, L., Schmid, R., Schwab, M.H., Lloyd, K.C., Eisenstat, D.D., Lai, C., and Anton, E.S. (2006). The role of neuregulin-ErbB4 interactions on the proliferation and organization of cells in the subventricular zone. Proc Natl Acad Sci U S A 103, 1930-1935.

Giachino, C., Basak, O., Lugert, S., Knuckles, P., Obernier, K., Fiorelli, R., Frank, S., Raineteau, O., Alvarez-Buylla, A., and Taylor, V. (2013). Molecular diversity subdivides the adult forebrain neural stem cell population. Stem Cells.

Giachino, C., and Taylor, V. (2009). Lineage analysis of quiescent regenerative stem cells in the adult brain by genetic labelling reveals spatially restricted neurogenic niches in the olfactory bulb. Eur J Neurosci 30, 9-24.

Gimeno, L., Corradi, A., Cobos, I., Consalez, G.G., and Martinez, S. (2004). Ezrin gene, coding for a membrane-cytoskeleton linker protein, is regionally expressed in the developing mouse neuroepithelium. Gene Expr Patterns 4, 749-754.

Gleeson, J.G., Lin, P.T., Flanagan, L.A., and Walsh, C.A. (1999). Doublecortin is a microtubule-associated protein and is expressed widely by migrating neurons. Neuron 23, 257-271.

Gonzalez-Perez, O., Romero-Rodriguez, R., Soriano-Navarro, M., Garcia-Verdugo, J.M., and Alvarez-Buylla, A. (2009). Epidermal growth factor induces the progeny of subventricular zone type B cells to migrate and differentiate into oligodendrocytes. Stem Cells 27, 2032-2043.

Graham, V., Khudyakov, J., Ellis, P., and Pevny, L. (2003). SOX2 functions to maintain neural progenitor identity. Neuron 39, 749-765.

Gritti, A., Bonfanti, L., Doetsch, F., Caille, I., Alvarez-Buylla, A., Lim, D.A., Galli, R., Verdugo, J.M., Herrera, D.G., and Vescovi, A.L. (2002). Multipotent neural stem cells reside into the rostral extension and olfactory bulb of adult rodents. J Neurosci 22, 437-445.

Hack, I., Bancila, M., Loulier, K., Carroll, P., and Cremer, H. (2002). Reelin is a detachment signal in tangential chain-migration during postnatal neurogenesis. Nat Neurosci 5, 939-945.

Hack, M.A., Saghatelyan, A., De Chevigny, A., Pfeifer, A., Ashery-Padan, R., Lledo, P.M., and Gotz, M. (2005). Neuronal fate determinants of adult olfactory bulb neurogenesis. Nat Neurosci 8, 865-872.

Hallberg, B., Rayter, S.I., and Downward, J. (1994). Interaction of Ras and Raf in intact mammalian cells upon extracellular stimulation. J Biol Chem 269, 3913-3916.

Harper, J.W., and Elledge, S.J. (2007). The DNA damage response: ten years after. Mol Cell 28, 739-745.

He, M., Zhao, M., Shen, B., Prise, K.M., and Shao, C. (2011). Radiation-induced intercellular signaling mediated by cytochrome-c via a p53-dependent pathway in hepatoma cells. Oncogene 30, 1947-1955.

Hellstrom, N.A., Bjork-Eriksson, T., Blomgren, K., and Kuhn, H.G. (2009). Differential recovery of neural stem cells in the subventricular zone and dentate gyrus after ionizing radiation. Stem Cells 27, 634-641.

Hellstrom, N.A., Lindberg, O.R., Stahlberg, A., Swanpalmer, J., Pekny, M., Blomgren, K., and Kuhn, H.G. (2011). Unique gene expression patterns indicate microglial contribution to neural stem cell recovery following irradiation. Mol Cell Neurosci 46, 710-719.

Hori, K., Sen, A., and Artavanis-Tsakonas, S. (2013). Notch signaling at a glance. J Cell Sci 126, 2135-2140.

Hu, H. (1999). Chemorepulsion of neuronal migration by Slit2 in the developing mammalian forebrain. Neuron 23, 703-711.

Hu, H., Tomasiewicz, H., Magnuson, T., and Rutishauser, U. (1996). The role of polysialic acid in migration of olfactory bulb interneuron precursors in the subventricular zone. Neuron 16, 735-743.

Hu, Q., Zhang, L., Wen, J., Wang, S., Li, M., Feng, R., Yang, X., and Li, L. (2010). The EGF receptor-sox2-EGF receptor feedback loop positively regulates the self-renewal of neural precursor cells. Stem Cells 28, 279-286.

Hubbard, B.M., and Hopewell, J.W. (1980). Quantitative changes in the cellularity of the rat subependymal plate after X-irradiation. Cell Tissue Kinet 13, 403-413.

Imayoshi, I., Sakamoto, M., Ohtsuka, T., Takao, K., Miyakawa, T., Yamaguchi, M., Mori, K., Ikeda, T., Itohara, S., and Kageyama, R. (2008). Roles of

continuous neurogenesis in the structural and functional integrity of the adult forebrain. Nat Neurosci 11, 1153-1161.

Iwamoto, R., Yamazaki, S., Asakura, M., Takashima, S., Hasuwa, H., Miyado, K., Adachi, S., Kitakaze, M., Hashimoto, K., Raab, G., Nanba, D., Higashiyama, S., Hori, M., Klagsbrun, M., and Mekada, E. (2003). Heparin-binding EGF-like growth factor and ErbB signaling is essential for heart function. Proc Natl Acad Sci U S A 100, 3221-3226.

Jackson, L.F., Qiu, T.H., Sunnarborg, S.W., Chang, A., Zhang, C., Patterson, C., and Lee, D.C. (2003). Defective valvulogenesis in HB-EGF and TACE-null mice is associated with aberrant BMP signaling. EMBO J 22, 2704-2716.

Jackson, S.P. (2002). Sensing and repairing DNA double-strand breaks. Carcinogenesis 23, 687-696.

Jen, Y., Manova, K., and Benezra, R. (1997). Each member of the Id gene family exhibits a unique expression pattern in mouse gastrulation and neurogenesis. Dev Dyn 208, 92-106.

Jerndal, M., Forsberg, K., Sena, E.S., Macleod, M.R., O'collins, V.E., Linden, T., Nilsson, M., and Howells, D.W. (2010). A systematic review and meta-analysis of erythropoietin in experimental stroke. J Cereb Blood Flow Metab 30, 961-968.

Johnson, M.W., Miyata, H., and Vinters, H.V. (2002). Ezrin and moesin expression within the developing human cerebrum and tuberous sclerosis-associated cortical tubers. Acta Neuropathol 104, 188-196.

Jones, R.B., Gordus, A., Krall, J.A., and Macbeath, G. (2006). A quantitative protein interaction network for the ErbB receptors using protein microarrays. Nature 439, 168-174.

Jorissen, R.N., Walker, F., Pouliot, N., Garrett, T.P., Ward, C.W., and Burgess, A.W. (2003). Epidermal growth factor receptor: mechanisms of activation and signalling. Exp Cell Res 284, 31-53.

Kahsai, A.W., Zhu, S., Wardrop, D.J., Lane, W.S., and Fenteany, G. (2006). Quinocarmycin analog DX-52-1 inhibits cell migration and targets radixin, disrupting interactions of radixin with actin and CD44. Chem Biol 13, 973-983.

Kaplan, M.S., and Hinds, J.W. (1977). Neurogenesis in the adult rat: electron microscopic analysis of light radioautographs. Science 197, 1092-1094.

Kim, Y., Comte, I., Szabo, G., Hockberger, P., and Szele, F.G. (2009). Adult mouse subventricular zone stem and progenitor cells are sessile and epidermal

growth factor receptor negatively regulates neuroblast migration. PLoS One 4, e8122.

Kinoshita, T., Nohata, N., Fuse, M., Hanazawa, T., Kikkawa, N., Fujimura, L., Watanabe-Takano, H., Yamada, Y., Yoshino, H., Enokida, H., Nakagawa, M., Okamoto, Y., and Seki, N. (2012). Tumor suppressive microRNA-133a regulates novel targets: moesin contributes to cancer cell proliferation and invasion in head and neck squamous cell carcinoma. Biochem Biophys Res Commun 418, 378-383.

Klempin, F., Kronenberg, G., Cheung, G., Kettenmann, H., and Kempermann, G. (2011). Properties of doublecortin-(DCX)-expressing cells in the piriform cortex compared to the neurogenic dentate gyrus of adult mice. PLoS One 6, e25760.

Koizumi, H., Higginbotham, H., Poon, T., Tanaka, T., Brinkman, B.C., and Gleeson, J.G. (2006). Doublecortin maintains bipolar shape and nuclear translocation during migration in the adult forebrain. Nat Neurosci 9, 779-786.

Kokovay, E., Goderie, S., Wang, Y., Lotz, S., Lin, G., Sun, Y., Roysam, B., Shen, Q., and Temple, S. (2010). Adult SVZ lineage cells home to and leave the vascular niche via differential responses to SDF1/CXCR4 signaling. Cell Stem Cell 7, 163-173.

Kondo, T., and Raff, M. (2000). The Id4 HLH protein and the timing of oligodendrocyte differentiation. EMBO J 19, 1998-2007.

Kuhn, H.G., Dickinson-Anson, H., and Gage, F.H. (1996). Neurogenesis in the dentate gyrus of the adult rat: age-related decrease of neuronal progenitor proliferation. J Neurosci 16, 2027-2033.

Kuhn, H.G., Winkler, J., Kempermann, G., Thal, L.J., and Gage, F.H. (1997). Epidermal growth factor and fibroblast growth factor-2 have different effects on neural progenitors in the adult rat brain. J Neurosci 17, 5820-5829.

Langlois, W.J., Sasaoka, T., Saltiel, A.R., and Olefsky, J.M. (1995). Negative feedback regulation and desensitization of insulin- and epidermal growth factor-stimulated p21ras activation. J Biol Chem 270, 25320-25323.

Lawson, L.J., Perry, V.H., Dri, P., and Gordon, S. (1990). Heterogeneity in the distribution and morphology of microglia in the normal adult mouse brain. Neuroscience 39, 151-170.

Lawson, L.J., Perry, V.H., and Gordon, S. (1992). Turnover of resident microglia in the normal adult mouse brain. Neuroscience 48, 405-415.

Lazarini, F., Gabellec, M.M., Torquet, N., and Lledo, P.M. (2012). Early activation of microglia triggers long-lasting impairment of adult neurogenesis in the olfactory bulb. J Neurosci 32, 3652-3664.

Lazarini, F., Mouthon, M.A., Gheusi, G., De Chaumont, F., Olivo-Marin, J.C., Lamarque, S., Abrous, D.N., Boussin, F.D., and Lledo, P.M. (2009). Cellular and behavioral effects of cranial irradiation of the subventricular zone in adult mice. PLoS One 4, e7017.

Le Belle, J.E., Orozco, N.M., Paucar, A.A., Saxe, J.P., Mottahedeh, J., Pyle, A.D., Wu, H., and Kornblum, H.I. (2011). Proliferative neural stem cells have high endogenous ROS levels that regulate self-renewal and neurogenesis in a PI3K/Akt-dependant manner. Cell Stem Cell 8, 59-71.

Lendahl, U., Zimmerman, L.B., and Mckay, R.D. (1990). CNS stem cells express a new class of intermediate filament protein. Cell 60, 585-595.

Li, Y.C., Park, M.J., Ye, S.K., Kim, C.W., and Kim, Y.N. (2006). Elevated levels of cholesterol-rich lipid rafts in cancer cells are correlated with apoptosis sensitivity induced by cholesterol-depleting agents. Am J Pathol 168, 1107-1118; quiz 1404-1105.

Liao, H., Huang, W., Niu, R., Sun, L., and Zhang, L. (2008). Cross-talk between the epidermal growth factor-like repeats/fibronectin 6-8 repeats domains of Tenascin-R and microglia modulates neural stem/progenitor cell proliferation and differentiation. J Neurosci Res 86, 27-34.

Ligon, K.L., Huillard, E., Mehta, S., Kesari, S., Liu, H., Alberta, J.A., Bachoo, R.M., Kane, M., Louis, D.N., Depinho, R.A., Anderson, D.J., Stiles, C.D., and Rowitch, D.H. (2007). Olig2-regulated lineage-restricted pathway controls replication competence in neural stem cells and malignant glioma. Neuron 53, 503-517.

Lin, C.F., Chen, C.L., and Lin, Y.S. (2006). Ceramide in apoptotic signaling and anticancer therapy. Curr Med Chem 13, 1609-1616.

Lois, C., and Alvarez-Buylla, A. (1994). Long-distance neuronal migration in the adult mammalian brain. Science 264, 1145-1148.

Lois, C., Garcia-Verdugo, J.M., and Alvarez-Buylla, A. (1996). Chain migration of neuronal precursors. Science 271, 978-981.

Luskin, M.B. (1993). Restricted proliferation and migration of postnatally generated neurons derived from the forebrain subventricular zone. Neuron 11, 173-189.

Marasas, W.F., Riley, R.T., Hendricks, K.A., Stevens, V.L., Sadler, T.W., Gelineau-Van Waes, J., Missmer, S.A., Cabrera, J., Torres, O., Gelderblom, W.C.,

Allegood, J., Martinez, C., Maddox, J., Miller, J.D., Starr, L., Sullards, M.C., Roman, A.V., Voss, K.A., Wang, E., and Merrill, A.H., Jr. (2004). Fumonisins disrupt sphingolipid metabolism, folate transport, and neural tube development in embryo culture and in vivo: a potential risk factor for human neural tube defects among populations consuming fumonisin-contaminated maize. J Nutr 134, 711-716.

Mercier, F., Kitasako, J.T., and Hatton, G.I. (2002). Anatomy of the brain neurogenic zones revisited: fractones and the fibroblast/macrophage network. J Comp Neurol 451, 170-188.

Merkle, F.T., Mirzadeh, Z., and Alvarez-Buylla, A. (2007). Mosaic organization of neural stem cells in the adult brain. Science 317, 381-384.

Merkle, F.T., Tramontin, A.D., Garcia-Verdugo, J.M., and Alvarez-Buylla, A. (2004). Radial glia give rise to adult neural stem cells in the subventricular zone. Proc Natl Acad Sci U S A 101, 17528-17532.

Mirzadeh, Z., Merkle, F.T., Soriano-Navarro, M., Garcia-Verdugo, J.M., and Alvarez-Buylla, A. (2008). Neural stem cells confer unique pinwheel architecture to the ventricular surface in neurogenic regions of the adult brain. Cell Stem Cell 3, 265-278.

Monje, M.L., Mizumatsu, S., Fike, J.R., and Palmer, T.D. (2002). Irradiation induces neural precursor-cell dysfunction. Nat Med 8, 955-962.

Monney, L., Olivier, R., Otter, I., Jansen, B., Poirier, G.G., and Borner, C. (1998). Role of an acidic compartment in tumor-necrosis-factor-alpha-induced production of ceramide, activation of caspase-3 and apoptosis. Eur J Biochem 251, 295-303.

Moreno, M.M., Linster, C., Escanilla, O., Sacquet, J., Didier, A., and Mandairon, N. (2009). Olfactory perceptual learning requires adult neurogenesis. Proc Natl Acad Sci U S A 106, 17980-17985.

Mouret, A., Gheusi, G., Gabellec, M.M., De Chaumont, F., Olivo-Marin, J.C., and Lledo, P.M. (2008). Learning and survival of newly generated neurons: when time matters. J Neurosci 28, 11511-11516.

Murray, P.J., and Wynn, T.A. (2011). Protective and pathogenic functions of macrophage subsets. Nat Rev Immunol 11, 723-737.

Murre, C., Mccaw, P.S., and Baltimore, D. (1989). A new DNA binding and dimerization motif in immunoglobulin enhancer binding, daughterless, MyoD, and myc proteins. Cell 56, 777-783.

Nagahara, A.H., and Tuszynski, M.H. (2011). Potential therapeutic uses of BDNF in neurological and psychiatric disorders. Nat Rev Drug Discov

10, 209-219.

Nagasawa, H., and Little, J.B. (1992). Induction of sister chromatid exchanges by extremely low doses of alpha-particles. Cancer Res 52, 6394-6396.

Nam, H.S., and Benezra, R. (2009). High levels of Id1 expression define B1 type adult neural stem cells. Cell Stem Cell 5, 515-526.

Narayanan, P.K., Goodwin, E.H., and Lehnert, B.E. (1997). Alpha particles initiate biological production of superoxide anions and hydrogen peroxide in human cells. Cancer Res 57, 3963-3971.

Neuman, T., Keen, A., Zuber, M.X., Kristjansson, G.I., Gruss, P., and Nornes, H.O. (1993). Neuronal expression of regulatory helix-loop-helix factor Id2 gene in mouse. Dev Biol 160, 186-195.

Newman, A.C., and Hughes, C.C. (2012). Macrophages and angiogenesis: a role for Wnt signaling. Vasc Cell 4, 13.

Nguyen-Ba-Charvet, K.T., Picard-Riera, N., Tessier-Lavigne, M., Baron-Van Evercooren, A., Sotelo, C., and Chedotal, A. (2004). Multiple roles for slits in the control of cell migration in the rostral migratory stream. J Neurosci 24, 1497-1506.

Nieto, M., Schuurmans, C., Britz, O., and Guillemot, F. (2001). Neural bHLH genes control the neuronal versus glial fate decision in cortical progenitors. Neuron 29, 401-413.

Ninomiya, M., Yamashita, T., Araki, N., Okano, H., and Sawamoto, K. (2006). Enhanced neurogenesis in the ischemic striatum following EGF-induced expansion of transit-amplifying cells in the subventricular zone. Neurosci Lett 403, 63-67.

Ono, K., Tomasiewicz, H., Magnuson, T., and Rutishauser, U. (1994). N-CAM mutation inhibits tangential neuronal migration and is phenocopied by enzymatic removal of polysialic acid. Neuron 13, 595-609.

Packer, R.J., Meadows, A.T., Rorke, L.B., Goldwein, J.L., and D'angio, G. (1987). Long-term sequelae of cancer treatment on the central nervous system in childhood. Med Pediatr Oncol 15, 241-253.

Paglini, G., Kunda, P., Quiroga, S., Kosik, K., and Caceres, A. (1998). Suppression of radixin and moesin alters growth cone morphology, motility, and process formation in primary cultured neurons. J Cell Biol 143, 443-455.

Palmer, T.D., Willhoite, A.R., and Gage, F.H. (2000). Vascular niche for adult hippocampal neurogenesis. J Comp Neurol 425, 479-494.

Parras, C.M., Galli, R., Britz, O., Soares, S., Galichet, C., Battiste, J., Johnson,

J.E., Nakafuku, M., Vescovi, A., and Guillemot, F. (2004). Mash1 specifies neurons and oligodendrocytes in the postnatal brain. EMBO J 23, 4495-4505.

Patra, S.K. (2008). Dissecting lipid raft facilitated cell signaling pathways in cancer. Biochim Biophys Acta 1785, 182-206.

Paxinos, G., and Watson, C. (2005). The rat brain in stereotaxic coordinates. Amsterdam ; Boston: Elsevier Academic Press.

Peretto, P., Giachino, C., Aimar, P., Fasolo, A., and Bonfanti, L. (2005). Chain formation and glial tube assembly in the shift from neonatal to adult subventricular zone of the rodent forebrain. J Comp Neurol 487, 407-427.

Persson, A., Lindberg, O.R., and Kuhn, H.G. (2013). Radixin inhibition decreases adult neural progenitor cell migration and proliferation in vitro and in vivo. Front Cell Neurosci 7, 161.

Persson, A., Lindwall, C., Curtis, M.A., and Kuhn, H.G. (2010). Expression of ezrin radixin moesin proteins in the adult subventricular zone and the rostral migratory stream. Neuroscience 167, 312-322.

Pineda, J.R., Daynac, M., Chicheportiche, A., Cebrian-Silla, A., Sii Felice, K., Garcia-Verdugo, J.M., Boussin, F.D., and Mouthon, M.A. (2013). Vascular-derived TGF-beta increases in the stem cell niche and perturbs neurogenesis during aging and following irradiation in the adult mouse brain. EMBO Mol Med 5, 548-562.

Prozorovski, T., Schulze-Topphoff, U., Glumm, R., Baumgart, J., Schroter, F., Ninnemann, O., Siegert, E., Bendix, I., Brustle, O., Nitsch, R., Zipp, F., and Aktas, O. (2008). Sirt1 contributes critically to the redox-dependent fate of neural progenitors. Nat Cell Biol 10, 385-394.

Quinones-Hinojosa, A., Sanai, N., Soriano-Navarro, M., Gonzalez-Perez, O., Mirzadeh, Z., Gil-Perotin, S., Romero-Rodriguez, R., Berger, M.S., Garcia-Verdugo, J.M., and Alvarez-Buylla, A. (2006). Cellular composition and cytoarchitecture of the adult human subventricular zone: a niche of neural stem cells. J Comp Neurol 494, 415-434.

Rakic, P. (1971). Neuron-glia relationship during granule cell migration in developing cerebellar cortex. A Golgi and electronmicroscopic study in Macacus Rhesus. J Comp Neurol 141, 283-312.

Ramón Y Cajal, S. (1928). Degeneration & regeneration of the nervous system. Oxford University Press, Humphrey Milford.

Reiss, G. (1992). Atypical cells in the normal guinea pig organ of Corti as revealed by micromanipulation in SEM. Microsc Res Tech 20, 288-297.

Reynolds, B.A., and Weiss, S. (1992). Generation of neurons and astrocytes from isolated cells of the adult mammalian central nervous system. Science 255, 1707-1710.

Roybon, L., Deierborg, T., Brundin, P., and Li, J.Y. (2009). Involvement of Ngn2, Tbr and NeuroD proteins during postnatal olfactory bulb neurogenesis. Eur J Neurosci 29, 232-243.

Ruzinova, M.B., and Benezra, R. (2003). Id proteins in development, cell cycle and cancer. Trends Cell Biol 13, 410-418.

Sahay, A., Scobie, K.N., Hill, A.S., O'carroll, C.M., Kheirbek, M.A., Burghardt, N.S., Fenton, A.A., Dranovsky, A., and Hen, R. (2011a). Increasing adult hippocampal neurogenesis is sufficient to improve pattern separation. Nature 472, 466-470.

Sahay, A., Wilson, D.A., and Hen, R. (2011b). Pattern separation: a common function for new neurons in hippocampus and olfactory bulb. Neuron 70, 582-588.

Sakamoto, M., Imayoshi, I., Ohtsuka, T., Yamaguchi, M., Mori, K., and Kageyama, R. (2011). Continuous neurogenesis in the adult forebrain is required for innate olfactory responses. Proc Natl Acad Sci U S A 108, 8479-8484.

Samanta, J., and Kessler, J.A. (2004). Interactions between ID and OLIG proteins mediate the inhibitory effects of BMP4 on oligodendroglial differentiation. Development 131, 4131-4142.

Sanai, N., Alvarez-Buylla, A., and Berger, M.S. (2005). Neural stem cells and the origin of gliomas. N Engl J Med 353, 811-822.

Sanai, N., Nguyen, T., Ihrie, R.A., Mirzadeh, Z., Tsai, H.H., Wong, M., Gupta, N., Berger, M.S., Huang, E., Garcia-Verdugo, J.M., Rowitch, D.H., and Alvarez-Buylla, A. (2011). Corridors of migrating neurons in the human brain and their decline during infancy. Nature 478, 382-386.

Sanai, N., Tramontin, A.D., Quinones-Hinojosa, A., Barbaro, N.M., Gupta, N., Kunwar, S., Lawton, M.T., Mcdermott, M.W., Parsa, A.T., Manuel-Garcia Verdugo, J., Berger, M.S., and Alvarez-Buylla, A. (2004). Unique astrocyte ribbon in adult human brain contains neural stem cells but lacks chain migration. Nature 427, 740-744.

Sandgren, E.P., Luetteke, N.C., Palmiter, R.D., Brinster, R.L., and Lee, D.C. (1990). Overexpression of TGF alpha in transgenic mice: induction of epithelial hyperplasia, pancreatic metaplasia, and carcinoma of the breast. Cell 61, 1121-1135.

Santana, P., Pena, L.A., Haimovitz-Friedman, A., Martin, S., Green, D.,

Mcloughlin, M., Cordon-Cardo, C., Schuchman, E.H., Fuks, Z., and Kolesnick, R. (1996). Acid sphingomyelinase-deficient human lymphoblasts and mice are defective in radiation-induced apoptosis. Cell 86, 189-199.

Sawamoto, K., Wichterle, H., Gonzalez-Perez, O., Cholfin, J.A., Yamada, M., Spassky, N., Murcia, N.S., Garcia-Verdugo, J.M., Marin, O., Rubenstein, J.L., Tessier-Lavigne, M., Okano, H., and Alvarez-Buylla, A. (2006). New neurons follow the flow of cerebrospinal fluid in the adult brain. Science 311, 629-632.

Schneider, M.R., and Wolf, E. (2008). The epidermal growth factor receptor and its ligands in female reproduction: insights from rodent models. Cytokine Growth Factor Rev 19, 173-181.

Schneider, M.R., and Wolf, E. (2009). The epidermal growth factor receptor ligands at a glance. J Cell Physiol 218, 460-466.

Seidenfaden, R., Desoeuvre, A., Bosio, A., Virard, I., and Cremer, H. (2006). Glial conversion of SVZ-derived committed neuronal precursors after ectopic grafting into the adult brain. Mol Cell Neurosci 32, 187-198.

Shao, C., Folkard, M., and Prise, K.M. (2008). Role of TGF-beta1 and nitric oxide in the bystander response of irradiated glioma cells. Oncogene 27, 434-440.

Shen, Q., Wang, Y., Kokovay, E., Lin, G., Chuang, S.M., Goderie, S.K., Roysam, B., and Temple, S. (2008). Adult SVZ stem cells lie in a vascular niche: a quantitative analysis of niche cell-cell interactions. Cell Stem Cell 3, 289-300.

Shihabuddin, L.S., Horner, P.J., Ray, J., and Gage, F.H. (2000). Adult spinal cord stem cells generate neurons after transplantation in the adult dentate gyrus. J Neurosci 20, 8727-8735.

Shirakata, Y., Kimura, R., Nanba, D., Iwamoto, R., Tokumaru, S., Morimoto, C., Yokota, K., Nakamura, M., Sayama, K., Mekada, E., Higashiyama, S., and Hashimoto, K. (2005). Heparin-binding EGF-like growth factor accelerates keratinocyte migration and skin wound healing. J Cell Sci 118, 2363-2370.

Sjostedt, S., and Bezak, E. (2010). Non-targeted effects of ionising radiation and radiotherapy. Australas Phys Eng Sci Med 33, 219-231.

Snapyan, M., Lemasson, M., Brill, M.S., Blais, M., Massouh, M., Ninkovic, J., Gravel, C., Berthod, F., Gotz, M., Barker, P.A., Parent, A., and Saghatelyan, A. (2009). Vasculature guides migrating neuronal precursors in the adult

mammalian forebrain via brain-derived neurotrophic factor signaling. J Neurosci 29, 4172-4188.

Spalding, K.L., Bergmann, O., Alkass, K., Bernard, S., Salehpour, M., Huttner, H.B., Bostrom, E., Westerlund, I., Vial, C., Buchholz, B.A., Possnert, G., Mash, D.C., Druid, H., and Frisen, J. (2013). Dynamics of hippocampal neurogenesis in adult humans. Cell 153, 1219-1227.

Suhonen, J.O., Peterson, D.A., Ray, J., and Gage, F.H. (1996). Differentiation of adult hippocampus-derived progenitors into olfactory neurons in vivo. Nature 383, 624-627.

Sultan, S., Mandairon, N., Kermen, F., Garcia, S., Sacquet, J., and Didier, A. (2010). Learning-dependent neurogenesis in the olfactory bulb determines long-term olfactory memory. FASEB J 24, 2355-2363.

Sun, D., Bullock, M.R., Altememi, N., Zhou, Z., Hagood, S., Rolfe, A., Mcginn, M.J., Hamm, R., and Colello, R.J. (2010). The effect of epidermal growth factor in the injured brain after trauma in rats. J Neurotrauma 27, 923-938.

Tada, E., Yang, C., Gobbel, G.T., Lamborn, K.R., and Fike, J.R. (1999). Long-term impairment of subependymal repopulation following damage by ionizing irradiation. Exp Neurol 160, 66-77.

Tavazoie, M., Van Der Veken, L., Silva-Vargas, V., Louissaint, M., Colonna, L., Zaidi, B., Garcia-Verdugo, J.M., and Doetsch, F. (2008). A specialized vascular niche for adult neural stem cells. Cell Stem Cell 3, 279-288.

Taylor, M.D., Poppleton, H., Fuller, C., Su, X., Liu, Y., Jensen, P., Magdaleno, S., Dalton, J., Calabrese, C., Board, J., Macdonald, T., Rutka, J., Guha, A., Gajjar, A., Curran, T., and Gilbertson, R.J. (2005). Radial glia cells are candidate stem cells of ependymoma. Cancer Cell 8, 323-335.

Tzeng, S.F. (2003). Inhibitors of DNA binding in neural cell proliferation and differentiation. Neurochem Res 28, 45-52.

Tzeng, S.F., Kahn, M., Liva, S., and De Vellis, J. (1999). Tumor necrosis factor-alpha regulation of the Id gene family in astrocytes and microglia during CNS inflammatory injury. Glia 26, 139-152.

Valderrama, F., Thevapala, S., and Ridley, A.J. (2012). Radixin regulates cell migration and cell-cell adhesion through Rac1. J Cell Sci 125, 3310-3319.

Van Furth, R., Cohn, Z.A., Hirsch, J.G., Humphrey, J.H., Spector, W.G., and Langevoort, H.L. (1972). The mononuclear phagocyte system: a new classification of macrophages, monocytes, and their precursor cells. Bull World Health Organ 46, 845-852.

Vandesompele, J., De Preter, K., Pattyn, F., Poppe, B., Van Roy, N., De Paepe, A., and Speleman, F. (2002). Accurate normalization of real-time quantitative RT-PCR data by geometric averaging of multiple internal control genes. Genome Biol 3, RESEARCH0034.

Vassar, R., and Fuchs, E. (1991). Transgenic mice provide new insights into the role of TGF-alpha during epidermal development and differentiation. Genes Dev 5, 714-727.

Ventura, R.E., and Goldman, J.E. (2007). Dorsal radial glia generate olfactory bulb interneurons in the postnatal murine brain. J Neurosci 27, 4297-4302.

Vescovi, A.L., Galli, R., and Reynolds, B.A. (2006). Brain tumour stem cells. Nat Rev Cancer 6, 425-436.

Vogin, G., and Foray, N. (2013). The law of Bergonie and Tribondeau: a nice formula for a first approximation. Int J Radiat Biol 89, 2-8.

Wahl, M.I., Nishibe, S., Kim, J.W., Kim, H., Rhee, S.G., and Carpenter, G. (1990). Identification of two epidermal growth factor-sensitive tyrosine phosphorylation sites of phospholipase C-gamma in intact HSC-1 cells. J Biol Chem 265, 3944-3948.

Walton, N.M., Sutter, B.M., Laywell, E.D., Levkoff, L.H., Kearns, S.M., Marshall, G.P., 2nd, Scheffler, B., and Steindler, D.A. (2006). Microglia instruct subventricular zone neurogenesis. Glia 54, 815-825.

Wang, C., Liu, F., Liu, Y.Y., Zhao, C.H., You, Y., Wang, L., Zhang, J., Wei, B., Ma, T., Zhang, Q., Zhang, Y., Chen, R., Song, H., and Yang, Z. (2011). Identification and characterization of neuroblasts in the subventricular zone and rostral migratory stream of the adult human brain. Cell Res 21, 1534-1550.

Wang, C.C., Liau, J.Y., Lu, Y.S., Chen, J.W., Yao, Y.T., and Lien, H.C. (2012). Differential expression of moesin in breast cancers and its implication in epithelial-mesenchymal transition. Histopathology 61, 78-87.

Wang, S., Sdrulla, A., Johnson, J.E., Yokota, Y., and Barres, B.A. (2001). A role for the helix-loop-helix protein Id2 in the control of oligodendrocyte development. Neuron 29, 603-614.

Weis, N., Weigert, A., Von Knethen, A., and Brune, B. (2009). Heme oxygenase-1 contributes to an alternative macrophage activation profile induced by apoptotic cell supernatants. Mol Biol Cell 20, 1280-1288.

Wilson, D.M., 3rd, Kim, D., Berquist, B.R., and Sigurdson, A.J. (2011). Variation in base excision repair capacity. Mutat Res 711, 100-112.

Winner, B., Cooper-Kuhn, C.M., Aigner, R., Winkler, J., and Kuhn, H.G. (2002). Long-term survival and cell death of newly generated neurons in the adult rat olfactory bulb. Eur J Neurosci 16, 1681-1689.

Wu, W., Wong, K., Chen, J., Jiang, Z., Dupuis, S., Wu, J.Y., and Rao, Y. (1999). Directional guidance of neuronal migration in the olfactory system by the protein Slit. Nature 400, 331-336.

Yarden, Y., and Sliwkowski, M.X. (2001). Untangling the ErbB signalling network. Nat Rev Mol Cell Biol 2, 127-137.

Young, K.M., Fogarty, M., Kessaris, N., and Richardson, W.D. (2007). Subventricular zone stem cells are heterogeneous with respect to their embryonic origins and neurogenic fates in the adult olfactory bulb. J Neurosci 27, 8286-8296.

Yun, K., Fischman, S., Johnson, J., Hrabe De Angelis, M., Weinmaster, G., and Rubenstein, J.L. (2002). Modulation of the notch signaling by Mash1 and Dlx1/2 regulates sequential specification and differentiation of progenitor cell types in the subcortical telencephalon. Development 129, 5029-5040.

Zhu, X., Morales, F.C., Agarwal, N.K., Dogruluk, T., Gagea, M., and Georgescu, M.M. (2013). Moesin is a glioma progression marker that induces proliferation and Wnt/beta-catenin pathway activation via interaction with CD44. Cancer Res 73, 1142-1155.

Ziv, Y., Ron, N., Butovsky, O., Landa, G., Sudai, E., Greenberg, N., Cohen, H., Kipnis, J., and Schwartz, M. (2006). Immune cells contribute to the maintenance of neurogenesis and spatial learning abilities in adulthood. Nat Neurosci 9, 268-275.

ACKNOWLEDGEMENTS

First and foremost I would like to express my deepest gratitude to my supervisor Georg Kuhn. I still remember our first meeting where you offered me a smörgåsbord of exciting projects at my picking. You opened my eyes to the wonderful world of science. Your openness and trust has made me a confident and independent scientist

Åsa Persson Sandelius for extremely fruitful collaborations and inspiring talks. You are a very talented researcher and it has been an honor working with you, and I truly hope we can continue our collaborations for years to come

Christi Cooper-Kuhn, my first supervisor at CBR who showed me the ropes. Your hard-working and thorough attitude is something I strive to reach myself

Anke Brederlau, you impress me with your enthusiasm and work ethic. I am really glad we got to work together and the papers in this thesis are better thanks to you

Giulia Zanni, You have played a great part in me keeping my sanity (almost) all the way through my PhD. Incredibly loyal, supportive, and an overall awesome person.

Reza Motalleb, for many laughs, great support, and late night UFC events in the lab

Former students of mine Aidin Shabro, Magdalena Rosinski, and Natasha Bank for valuable contributions to this thesis

Former members of the Kuhn group: Ahmed Osman, Axel Jansson, Nina Erkenstam, and Jenny Zhang for creating a great working environment, fruitful collaborations, and making me feel right at home when I first started out

Birgit Linder and Ann-Marie Alborn you are two of the most amazing persons I have ever met. I am forever deeply grateful for your unquestionable support. It has been a privilege working with you. I will miss your warmth and technical excellence